UNIVERSITY OF PLYMOUTH

making space for sand

Building Community Resilience on a Dynamic Coast by Making Space for Sand | MS4S

DELIVERABLE 1: CONTEMPORARY DUNE EVOLUTION AND FUTURE PREDICTIONS



Report provided by: University of Plymouth

Report provided for: Cornwall Council

Date: 08/03/2024

Document version: MS4S_D1V3

DISCLAIMER

Whilst UoP will use all reasonable endeavours to ensure the accuracy of the work performed and any information given, UoP makes no warranty, express or implied, as to accuracy and will not be held responsible for any consequence arising out of any inaccuracies or omissions unless such inaccuracies or omissions are the result of negligence on the part of UoP or its agents.

The obligations of UoP and its agents shall cease upon delivery of the report and no liability whatsoever either direct or indirect shall rest upon them for the effects of any product or process that may be produced or adopted by the client or any other party, notwithstanding that the formulation of such product or process may be based upon the findings of the report.

UoP shall not be liable for any death or injury unless it is caused by the negligence of UoP or its agents, nor shall it be liable for any loss or damage whatsoever unless it is caused by its wilful default or that of its agents.

UNIVERSITY OF PLYMOUTH

making space for sand

Document Information

Document permissions	Cornwall Council
Project name	Building Community Resilience on a Dynamic Coast by Making Space for Sand: Deliverable 1: Contemporary Dune Evolution and Future Predictions
Report date	8th March 2024
Document Version	MS4S_D1V4
Client	Cornwall Council
Client representative	Jolyon Sharpe
Academic lead	Prof. Gerd Masselink
Project manager	Aikaterini Konstantinou
Consultant(s)	Liane Brodie, Christopher Stokes
Report Citation	CMAR, 2023. MS4S: Contemporary Dune Evolution and Future Predictions, Report, University of Plymouth, 129 pp.

Document history

Date	Issue	Prepared	Approved	Authorised	notes
21/08/23	MS4S_D1V1	LB	AK & CS	GM	
17/11/23	MS4S_D1V2	LB	CS	GM	
08/03/2024	MS4S_D1V3	AK/LB	AK	GM	

Document authorisation

Prepared	Approved	Authorised
		
Liane Brodie	Aikaterini Konstantinou	Prof. Gerd Masselink

MS4S: Contemporary Dune Evolution and Future Predictions

Executive Summary

Coastal dunes are dynamic features that form the first line of defence against flooding and provide important ecological and socio-economic benefits to communities. Coastal dunes are vulnerable to changes in sea level and storminess and are expected to experience increased erosion with climate change. Historical patterns of dune evolution can provide important insights into coastal resilience that can be used to inform predictions of future morphological changes. Dune dynamics for 40 sites in Cornwall, UK (Figure 1-1), were investigated by analysing airborne LiDAR data over a 12-year period (2007 – 2020), forming the initial site characterisation for the DEFRA funded 'Building Community Resilience on a Dynamic Coast by Making Space for Sand' (MS4S) project. The principal aims of this study are to quantify contemporary dune dynamics (12-year period) and make projections of possible future dune evolution at each site.

Contemporary dune evolution was quantified in two ways: (1) horizontal dune toe change (δX), which indicates whether the base of a dune system is retreating/advancing; and (2) dune volumetric change (δQ), which indicates whether the sediment volume associated with a dune system is increasing/decreasing. Results indicate that over the 12-year period about half the sites have lost volume and half have gained volume. Despite some dune systems increasing in volume, the majority (58%) have retreated over this period, suggesting a change in the geometry of the dune profile. More than half the dunes show signs of rollover (where sediment is accreting on top of the dune), although in many cases this is outpaced by erosion of the dune front. However, because of significant variability (increases and decreases) in dune morphology over time, only eight sites have a statistically significant temporal trend in δX and/or δQ. Three main dune behaviours are observed:

1) Dunes that are gaining sediment and advancing, which are likely dominated by aeolian (wind-driven) sediment transport from the beach into the dunes (n = 3)
2) Dunes that are losing sediment and retreating, which are likely dominated by storm erosion (n = 4)
3) Dunes that are gaining sediment and retreating, exhibiting what is referred to as roll-over, which are likely dominated by storm erosion of the frontal dune and aeolian sediment transported from the beach and dune front to the top and back of the dune (n =1).

Future projections of dune evolution were made by: (1) extrapolating contemporary changes in the position of the dune toe; and (2) applying the widely used Bruun rule to translate the dune toe landward

with sea level rise. As significant trends in δX were only observed at a small number (8) of sites, the former approach (extrapolation of contemporary dune toe changes) is of limited use. Where statistically significant trends in δX were observed, extrapolation of these trends leads to estimates of dune toe retreat/advance >100 m by 2100. However, this approach assumes that current observed trends are representative over a multi-decadal timescale and will continue unchanged into the future, which is unlikely.

Bruun rule estimates of dune retreat by 2100 at all sites range between 13 m and 61 m. These projections are, however, limited in the processes they account for, neglecting longshore sediment transport, aeolian sediment transport, and underlying geology/sediment availability, and have underpredicted dune changes over the contemporary period studied. Therefore, projections of future dune evolution presented in this report represent a first-stage assessment of future dune behaviour in Cornwall and have identified important opportunities to improve these projections in further work. Subsequent analysis for the Making Space for Sand project will include the development and application of more advanced models of dune evolution, which will combine models of sea level response, storm wave erosion, aeolian sand transport, and sediment availability.

Contents

1. Introduction 1

1.1. Study Approach 1

1.2. Description of Dune Sites, Tide, Wind and Wave Climate 1

2. Methodology 6

2.1. Contemporary Dune Evolution 6

2.1.1. Dune Toe Change (δX) 6

2.1.2. Dune Volume Change (δQ) 10

2.2. Projections of Future Change 11

2.2.1. Future Projections Using Contemporary Trends 12

2.2.2. Bruun Rule Projections 12

2.2.3. Contemporary Bruun Rule Predictions 16

2.2.4. Assumptions and Limitations 16

3. Results 17

3.1. Contemporary Dune Evolution 17

3.1.1. Temporal trends of dune morphology 17

3.1.2. Comparison of contemporary rates of dune toe change 25

3.2. Projected Future Change 28

3.2.1. Future Projections Using Contemporary Trends 28

3.2.2. Future Bruun Rule Projections 29

3.3. Caveats 31

4. Conclusion 33

References 35

Appendix A. LiDAR data collection years 37

Appendix B. 2100 Projected Retreat using Contemporary Rates and the Bruun Rule 38

Appendix C. Changes in dune volume and dune foot position observed over the survey period (2007/2009 to 2019/2020) 39

Appendix D. 2100 Projected Bruun Rule and Elevation Change Maps 40

Table of Figures

Figure 1-1. Locations and names of the 40 project sites across Cornwall. Wave roses of significant wave heights Hs are from model nodes offshore of Holywell, Praa Sands and Caerhays (from the Met Office Wave Watch III model hindcast, Atlantic-European North West Shelf-Wave Physics Reanalysis https://doi.org/10.48670/moi-00060)..... 3

Figure 1-2. Example of four sites with aerial images (left) and images of the side dune profile (right). Blue lines on the aerial photography outline the 'Mobile Zone' over which dune volume has been calculated. Red triangles indicate the approximate field of view of each of the right panel photos. Site examples are Crantock (top), and Mexico Towans (second from top) on the northern coastline and Marazion (second from bottom) and Par Sands (bottom) on the southern coastline. 4

Figure 2-1. Estimated dune toe elevation at each site (m ODN). Sites to the left (right) of the red line are on the southern (northern) coast of Cornwall. 7

Figure 2-2. Change in dune toe position (δX) relative to the 2008 LiDAR survey at Par Sands (black dots). Error bars show the longshore standard deviation in δX and the regression line describing the dune toe trend is shown in red. 8

Figure 2-3. Change in dune volume (δQ) relative to the first (here 2008) LiDAR survey at Par Sands (black dots). Error bars show the LiDAR measurement error and the regression line describing the dune toe trend is shown in red. 10

Figure 2-4. UKCP18 predictions of relative sea-level rise (SLR) at Seaton under high, medium, and low emissions scenarios (from https://ukclimateprojections-ui.metoffice.gov.uk/). Lower (5th percentile), median (50th percentile), and upper (95th percentile) predictions are also shown for each scenario, indicating the magnitude of uncertainty, determined from an ensemble of UKCP18 model predictions..... 11

Figure 2-5. Schematic of Bruun rule showing current equilibrium beach profile and future profile due to sea level rise (from Cooper & Pilkey, 2004). Where B is the berm height, W_* is the width of active shoreface, and h_* is the morphological depth of closure..... 12

Figure 2-6. Example of longshore distribution of the height of the shoreface ($h* + B$) (left) and width of the shoreface ($W*$) (right) at Par Sands..... 14

Figure 3-1. Time series of dune toe migration relative to the first LiDAR survey (δX) for the 40 sites (black dots). A negative change represents retreat, and a positive change represents advance. Black error bars show the longshore standard deviation, and the red line is the linear fit (trend line). Site names with a statistically significant trend (p-values < 0.05) are displayed in orange for retreating sites and blue for advancing sites. * indicates sites without dunes. The green dashed lines mark the

winter of 2013/14, the most energetic winter in at least 65 years (Masselink et al., 2016). Magenta shading show periods over which significant volume changes have occurred at Lelant Towams, Crantock and Rock Dune discussed in this section..... 18

Figure 3-2. Time series of dune volume change (m^3/m) relative to the first LiDAR survey (δQ) for the 40 sites (black dots). A negative change represents volume loss and a positive change volume gain. Black error bars show the LiDAR measurement error, and the red line is the linear fit (trend line). Site names with a statistically significant trend (p-values < 0.05) are displayed in orange for eroding sites and blue for accreting sites. * indicates sites without dunes. The green dashed lines show the winter of 2013/14, the most energetic winter in at least 65 years (Masselink et al., 2016)). Magenta shading show periods over which significant volume changes have occurred at Lelant Towams, Crantock and Rock Dune discussed in this section..... 19

Figure 3-3. Sediment volume gains (blue) vs losses (red) for the 34 dune sites in the study region over the study period..... 20

Figure 3-4. Spatial representation of dune changes observed over the LiDAR survey period for the 40 MS4S sites. Volume change per meter dune width above the dune toe (left); and dune toe migration (δX) (right). Volume loss and dune toe retreat are shown in orange and volume gain and dune toe advance are shown in blue. These results are presented analytically in Table 3-1..... 21

Figure 3-5. Relationship between the rate of dune volumetric change $\delta Q/\delta T$ and the rate of dune toe change $\delta X/\delta T$ for the 11/12-year monitoring period for all sites. Sites with absolute $\delta X/\delta T$ rates larger than 1m/yr are labelled..... 21

Figure 3-6. Relationship between the rate of dune volumetric change $\delta Q/\delta T$ and the rate of dune toe change $\delta X/\delta T$ (left) and the values of $\delta Q/\delta T$ and $\delta X/\delta T$ for each site (right) over the survey period. Only sites with a statistically significant trend in volume and toe position were included. Highlighted in blue are sites that are gaining sediment and advancing, in orange are sites that are losing sediment and retreating, and in yellow the one site that is gaining sediment and retreating. 22

Figure 3-7. (A) Observed rates of dune toe change calculated from the gradient of the linear trend line ($\delta X/\delta T$), (B) from the change in dune toe from the first to last survey $\delta X_{last\text{-}first}/\delta T$, and (C) Bruun rule rates estimated for the past 15 years of SLR observed at Newlyn. Positive results indicate dune toe advance and negative results indicate dune toe retreat. 26

Figure 3-8. 2100 predicted retreat (m) for the 40 sites using observed rates of change based on two methods: (1) the gradient of the linear trend line ($\delta X/\delta T$); and (2) the change in dune toe from the first to last survey ($\delta X_{last\text{-}first}/\delta T$). Negative results are for dune toe retreat and positive trends are for dune toe advance. Sites names with significant trends are highlighted in red (for negative trends) and blue (for positive trends)..... 28

Figure 3-9. Contemporary dune toe change over the survey period (blue) and Bruun rule projected future change (orange) to the year 2100 relative to the last LiDAR survey for the 40 Cornish dune sites. Positive results indicate dune toe advance and negative results indicate dune toe retreat. Sites names with a statistically significant (p-values < 0.05) historic trend are displayed in orange for retreating sites and blue for advancing sites. * indicates sites without dunes. 30

Figure 3-10. 2100 predicted retreat (m) for the 40 sites using the probabilistic Bruun rule approach (detailed in Section 2.2.2). Negative results indicate dune toe retreat. Red bars indicate median (50%) estimate, and the error bars represent 5th and 95th percentile values. 31

Figure C-1. Changes in dune volume (x-axis) and location of the dune foot (y-axis) extracted between the first available LiDAR survey (2007 to 2009 depending on the site) and last available LiDAR data (2019 to 2020 depending on the site). a). all sites; b). same plot zoomed in to the area highlighted by the red, dashed line rectangle in (a). c). same plot zoomed in to the area highlighted by the green, dash-dot line rectangle in (a) and (b). The dates of the first and last LiDAR data available are provided in Table A-1 and the corresponding dune foot change and volume change values are included in Table 3-1. 39

Table of Tables

Table 1-1. Site characteristics table including whether the site is considered to have dunes or not, area of the 'Mobile Zone', the length of the dune system, tidal range, and median significant wave height at break point (H_b). 5

Table 2-1. Site characteristics used within the Stockdon equation, including Ho, Lo, and longshore median βf for the 2019/20 epoch as well as the calculated dune toe elevation for each site in m above Ordinance Datum Newlyn (ODN). 9

Table 2-2. Parameters used for the Bruun rule projections, including depth of closure (m ODN), median berm height, longshore median shoreface and longshore median height of the shoreface. 15

Table 3-1. Net volume change per meter dune width above the dune toe (δQlast-first) and net dune toe migration (δXlast-first) observed over the LiDAR survey period. 27

Table 3-2. Rates of change derived from linear regression *(δX/δT*, *δQ/δT)* and associated p-values for all sites. Negative trends signify retreat of the dune toe (δX/δT) and loss of dune volume (δQ/δT) respectively appear in red. Statistically significant (p < 0.05) trends, wither positive or negative, are highlighted in bold font. 24

Table 3-3. Rates of dune toe change calculated from the gradient of the linear trend line *δX/δT* and from *δX* calculated from the last survey *δXlast-first/δT*, as well as Bruun rule rates estimated for

the past 15 years of SLR observed at Newlyn. Sites with statistically significant advancing trends are highlighted in blue and those with statistically significant retreating trends in red. 27

Table A-1. First and last LiDAR survey dates. 37

Table B-1. Values of the estimated 2100 retreat using the two contemporary rate estimates (*δX/δT* and δXlast-first*/δT)* and using the Bruun rule. Sites with statistically significant advancing trends are highlighted in blue and those with statistically significant retreating trends in red. 38

1. Introduction

This analysis forms the initial site characterisation for the DEFRA funded and EA managed Flood and Coastal Resilience Innovation Programme through the 'Building Community Resilience on a Dynamic Coast by Making Space for Sand' project (MS4S). The principal aims of this study is to quantify the contemporary dune dynamics and estimate possible future dune evolution at each site.

1.1. Study Approach

Dune dynamics for 40 sites in Cornwall, UK (Figure 1-1), were investigated by analysing airborne LiDAR data over a 12-year period. Contemporary dune evolution was quantified from the LiDAR data in two ways:

- **Dune toe change (δX)** – refers to the alongshore-averaged change in the cross-shore location of the dune toe (defined in Section 2.1.1) and is used to estimate the rate of dune toe change ($\delta X/\delta T$) over the 11/12-year survey period.
- **Volume change (δQ)** – refers to the alongshore-averaged change in the dune volume within a specified area termed the 'mobile zone' (i.e., the area over which the dune system is considered to be mobile) over the survey period (2007/09 and 2019/20). δQ is used to derive the observed rate of volume change ($\delta Q/\delta T$) over the 11/12-year survey period.

Future change in the dune toe position was then projected using either Bruun rule estimates or extrapolation of contemporary dune toe changes using observed trends, where these could be identified.

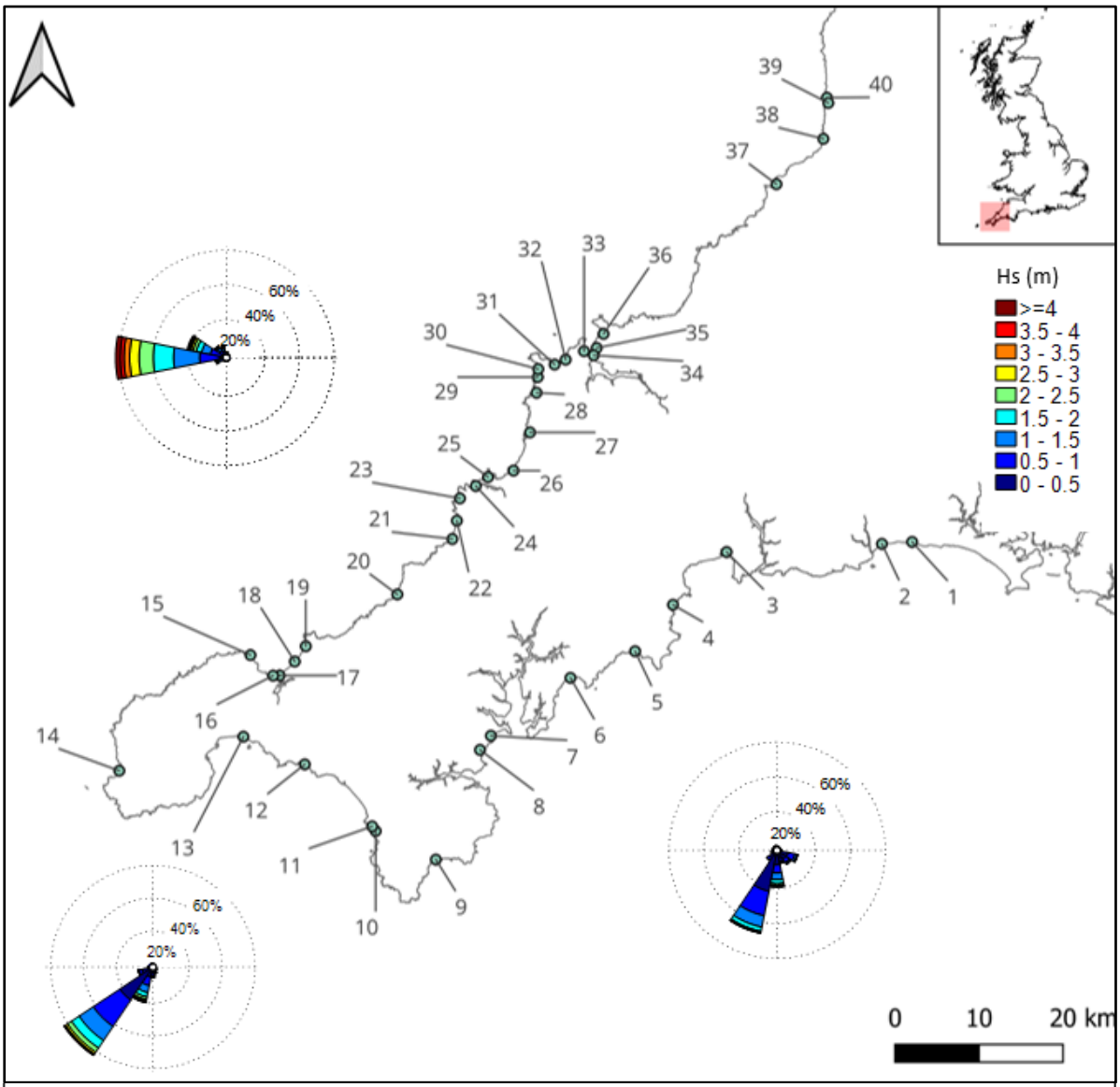
Of the 40 MS4S sites, nine do not currently have developed dune systems (detailed in Table 1-1). It is important to note that the results for these sites will be related to changes to the upper beach. However, for the benefit of consistency, the terminology used in this report for all sites is 'dune toe change' and 'dune volume change'.

1.2. Description of Dune Sites, Tide, Wind and Wave Climate

The 40 dune sites across the Cornish peninsula (Figure 1-1) exhibit great diversity in morphological type, size, orientation, and hydrodynamic conditions. Figure 1-2 includes four examples illustrating the range of dune types found in the region: Crantock and Mexico Towans on the northern coastline, and Marazion and Par Sands on the southern coastline. Southern dunes tend to be smaller and lower compared to most of their northern counterparts. The majority of the sites are bay dunes, where the supply of sand is trapped within two headlands (Radley, 1994), and some of these systems also have a significant estuarine or riverine influence, e.g., Crantock (Figure 1-2), Hawkers Cove and Rock Dune. Many of the northern dune sites, and some at the southern tip of Cornwall, are so-called 'climbing dunes' where a cliff or other form of bedrock underlies an often shallow dune deposit (Masselink et al., 2022; Radley, 1994). Several MS4S sites do not currently have developed dune systems while others

have extensive dune systems with large man-made developments (e.g., car parks, golf courses) on the dunes.

The hydrodynamic conditions along the coast vary considerably with the northern coast experiencing larger, predominantly westerly waves, with a 1% exceedance significant wave height ($H_{s1\%}$) of 5.0 m compared with the smaller, predominantly south-westerly waves on the southwest facing coast ($H_{s1\%}$= 3.4 m), and more moderate south-south-westerly waves on the sheltered southeast facing coast ($H_{s1\%}$= 2.4 m) (Figure 1-1). Significant wave heights at breaker point (H_b) range from 0.1 m at Maenporth (south coast) to 1.8 m at Sennen (west coast) and are provide in Table 1-1 as indicators of local nearshore wave conditions. Wind speed observations on the north coast (at Site 21 - Perranporth) indicate dominant westerly winds with an average wind speed of 5.6 m/s, while the south coast experiences milder winds (average 2.6 m/s) primarily form a west-southwest direction (at Site 1 - Seaton) (www.windfinder.com). The spring tide range increases from 4.8 m at Site 1 (Seaton) on the south coast to 6.4 m at Site 40 (Crooklets) on the north coast. Details of the characteristics of the MS4S sites are presented in Table 1-1 and include tidal characteristics and wave conditions. Table 1-1 also includes the size of the 'Mobile Zone', defined at each site as the area between the MHWS contour and a fixed landward location where the dune system is considered to be mobile (examples in Figure 1-2), and the length of the dune system, defined as the length of the most seaward MHWS contour extracted from the LiDAR data. It is further noted that nine sites are not considered to have any dunes associated with them; these are also indicated in Table 1-1.



1	Seaton	9	Kennack Sands	17	Harveys Towans	25	Fistral Beach	33	Hawkers Cove
2	Milendreath	10	Poldhu Cove	18	Mexico Towans	26	Porth	34	Rock Dune
3	Par Sands	11	Church Cove	19	Gwithian Towans	27	Mawgan Porth	35	Daymer Bay
4	Pentewan	12	Praa Sands	20	Porthtowan	28	Porthcothan	36	Polzeath
5	Caerhays	13	Marazion	21	Perranporth	29	Treyarnon Bay	37	Crackington Haven
6	Pendower	14	Sennen Cove	22	Penhale	30	Constantine Bay	38	Widemouth Bay
7	Swanpool	15	Porthmeor	23	Holywell	31	Harlyn	39	Summerleaze
8	Maenporth	16	Lelant Towans	24	Crantock	32	Trevone	40	Crooklets

Figure 1-1. Locations and names of the 40 project sites across Cornwall. Wave roses of significant wave heights Hs are from model nodes offshore of Holywell, Praa Sands and Caerhays (from the Met Office Wave Watch III model hindcast, Atlantic-European North West Shelf-Wave Physics Reanalysis https://doi.org/10.48670/moi-00060).



Figure 1-2. Example of four sites with aerial images (left) and images of the side dune profile (right). Blue lines on the aerial photography outline the 'Mobile Zone' over which dune volume has been calculated. Red triangles indicate the approximate field of view of each of the right panel photos. Site examples are Crantock (top), and Mexico Towans (second from top) on the northern coastline and Marazion (second from bottom) and Par Sands (bottom) on the southern coastline.

Table 1-1. Site characteristics table including whether the site is considered to have dunes or not, area of the 'Mobile Zone', the length of the dune system, tidal range, and median significant wave height at break point (H_b).

Site Name	Dune/ Not Dune	Area of Mobile Zone (m^2)	Length of dune system (m)	Spring tidal range (m)	Mean tidal range (m)	Median significant wave heights at break point (H_b m)
Southern Coast						
Seaton	Not Dune	23,097	476	4.8	3.50	0.6
Milendreath	Not Dune	3,500	167	4.8	3.50	0.7
Par Sands	Dune	3,500	900	4.5	3.35	0.4
Pentewan	Dune	42,713	930	4.7	3.50	0.4
Caerhays	Dune	4,308	137	4.6	3.40	0.5
Pendower	Dune	6,964	155	4.6	3.40	0.5
Swanpool	Not Dune	3,590	167	4.6	3.40	0.4
Maenporth	Dune	8,429	204	4.6	3.40	0.1
Kennack Sands	Dune	16,191	685	4.7	3.50	0.7
Poldhu Cove	Dune	11,745	138	4.7	3.50	1.3
Church Cove	Dune	17,323	176	4.7	3.50	1.1
Praa Sands	Dune	80,617	1,746	4.7	3.50	0.8
Marazion	Dune	67,813	1,734	4.8	3.60	0.6
Northern Coast						
Sennen Cove	Dune	101,206	2,513	4.8	3.60	1.8
Porthmeor	Not Dune	30,489	555	5.8	4.15	1.4
Lelant Towans	Dune	50,678	976	5.8	4.15	0.8
Harveys Towans	Dune	96,370	999	5.8	4.15	1.1
Mexico Towans	Dune	321,458	2,964	5.8	4.15	1.1
Gwithian Towans	Dune	108,295	634	5.8	4.15	1.5
Porthtowan	Dune	13,537	233	5.8	4.15	1.5
Perranporth	Dune	75,837	376	6.2	4.40	1.5
Penhale	Dune	107,581	1,590	6.1	4.40	1.6
Holywell	Dune	71,941	672	6.1	4.40	1.6
Crantock	Dune	93,538	921	6.4	4.60	1.4
Fistral Beach	Dune	35,822	703	6.4	4.60	1.6
Porth	Not Dune	34,836	222	6.4	4.60	1.3
Mawgan Porth	Dune	16,870	337	6.5	4.60	1.4
Porthcothan	Dune	15,730	141	6.4	4.60	1.6
Treyarnon Bay	Dune	7,652	153	6.4	4.60	1.7
Constantine Bay	Dune	43,689	683	6.4	4.60	1.7
Harlyn	Dune	13,431	248	6.5	4.75	1.2
Trevone	Not Dune	4,989	123	6.5	4.75	1.3
Hawkers Cove	Dune	47,591	603	6.5	4.75	0.3
Rock Dune	Dune	181,770	1,098	6.5	4.75	1.0
Daymer Bay	Dune	19,735	403	6.5	4.75	1.1
Polzeath	Not Dune	27,768	290	6.5	4.75	1.3
Crackington Haven	Not Dune	6,168	187	6.4	4.65	1.5
Widemouth Bay	Dune	66,374	1,019	6.4	4.65	1.5
Summerleaze	Dune	29,770	222	6.4	4.65	1.2
Crooklets	Not Dune	6,432	185	6.4	4.65	1.4

2. Methodology

2.1. Contemporary Dune Evolution

Airborne Light Detection And Ranging (LiDAR) data with a vertical accuracy of 15 cm were used to create high-resolution digital elevation models (DEMs) of ground elevation at each of the study sites. LiDAR data is available for the years 2007 to 2020 (referred to herein as the survey period) and is provided by the South West Coastal Monitoring Programme (SWCMP; https://southwest.coastalmonitoring.org/). It should be noted that LiDAR data is not captured concurrently at all MS4S sites. The dates of the first and last available LiDAR data at each site are provided in Table A-1. The DEMs were used to determine the location of the dune toe and derive changes in dune toe location and dune volume between epochs. The first and last LiDAR surveys for each site are detailed in Appendix A.

2.1.1. Dune Toe Change (δX)

The 'dune toe' separates the beach area from the dune region and is often used to map and track dune dynamics (Ruessink & Jeuken, 2002; van IJzendoorn et al., 2021). This transition between the beach and dune is often defined as a set elevation on the beach profile. For this study, the dune toe elevation was determined for each of the studied dune systems as the sum of the Mean High Water Spring (MHWS) level and the wave runup height during 1% exceedance waves (e.g., extreme storm), which represents the vertical limit of the beach profile typically influenced by wave action.

The wave runup elevation was determined using the formulations proposed by Stockdon et al. (2006). The authors define two equations for estimating runup depending on the wave breaking regimes (spilling, plunging, or surging) as described by the Iribarren number (Battjes, 1974):

$$\xi = \frac{\beta_f}{(H_0/L_0)^{1/2}}$$

where β_f is the foreshore slope, H_0 the deep-water wave height and L_0 is the deep-water wavelength. Once ξ has been defined, the Stockdon equations are expressed as:

$$R_2 = 0.043(H_0 L_0)^{1/2} \text{ for } \xi < 0.3$$

and

$$R_2 = 1.1\left(0.35\beta_f(H_0 L_0)^{1/2} + \frac{[H_0 L_0(0.563\beta_f{}^2 + 0.004)]^{1/2}}{2}\right) \text{ for } \xi > 0.3$$

where R_2 is the 2% runup exceedance value.

Wave data were obtained from the Met Office Wave Watch III model hindcast, Atlantic-European North West Shelf-Wave Physics Reanalysis (https://doi.org/10.48670/moi-00060) model, which has a 1.5 km spatial resolution. Data were extracted at the closest model node directly offshore of the dune system. As the deep-water wavelength is required for the above equations, the wave data were first shoaled and refracted to the point of theoretical wave breaking using linear shoaling and refraction equations, then reverse shoaled out to 1000 m water depth to obtain the deep-water wave height values (H_0). The deep-water wavelength (L_0) used in the runup equation was calculated based on the 1% exceedance H_0.

The dune toe elevation (MHWS + R_2) was calculated along profiles extracted every 10 m along the MHWS contour extracted from the first and last available LiDAR data at each site. The value of R_2 was estimated based on the foreshore slope (β_f) computed between MHWS - $\frac{H_0}{2}$ and MHWS + $\frac{H_0}{2}$ (at each profile and for the first and last epoch), based on the 1% exceedance H_0. The longshore median values obtained for each epoch where then averaged to define the dune toe elevation at each site. Figure 2-1 details the resulting values of the dune toe elevation, while Table 2-1 also includes the variables used in the Stockdon equation.

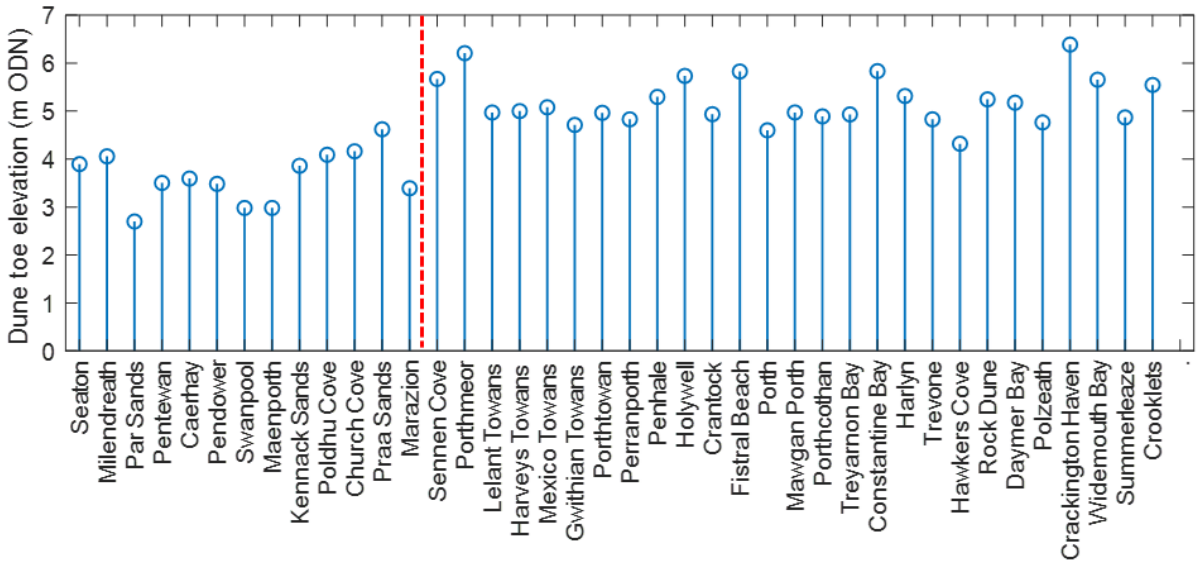


Figure 2-1. Estimated dune toe elevation at each site (m ODN). Sites to the left (right) of the red line are on the southern (northern) coast of Cornwall.

The cross-shore change in dune toe position was determined at each profile between each available LiDAR survey and the first survey, yielding a longshore distribution of dune toe change. From this, the median longshore change in dune toe position (δX) was calculated at each site. A linear regression was fitted to the time series of δX to evaluate any trends in dune toe position. An f-test was used to determine

the statistical significance of the observed trends (i.e., whether the observed trends can be considered real and not due to random noise) and only trends with p-values < 0.05 (i.e., 95% confidence) were considered statistically significant. The rates of dune toe change ($\delta X/\delta T$) were then calculated as the gradient of the fitted regression line. Figure 2-2 shows an example of the time series of δX for Par Sands, which exhibits a statistically significant trend ($p < 0.05$), reflecting a progressively prograding dune toe, represented by the fitted linear regression line (in red). The results for all sites are presented in Section 3.1.1. A second method was used to calculate dune toe change rates for each site by simply taking δX of the final survey year and dividing by the number of years between first and last survey ($\delta X_{last\text{-}first}/\delta T$). These results are presented in Section 3.1.2.

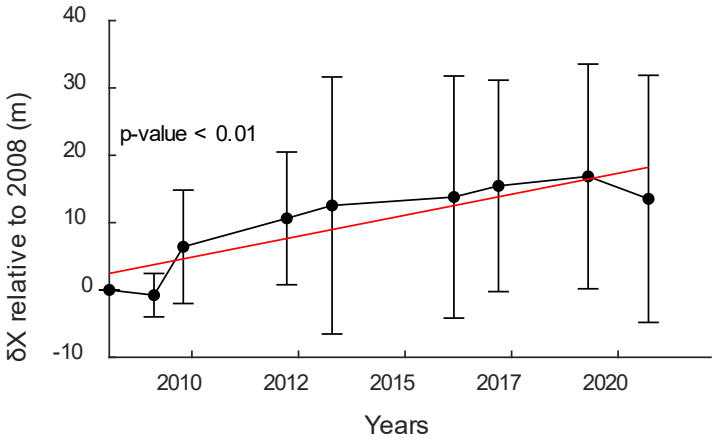


Figure 2-2. Change in dune toe position (δX) relative to the 2008 LiDAR survey at Par Sands (black dots). Error bars show the longshore standard deviation in δX and the regression line describing the dune toe trend is shown in red.

Table 2-1. Site characteristics used within the Stockdon equation, including H_o, L_o, and longshore median β_f for the 2019/20 epoch as well as the calculated dune toe elevation for each site in m above Ordinance Datum Newlyn (ODN).

Site Name	H_0 (m) –1% exceedance	L_0 (m)	Longshore median β_f in 2019/20 (m)	MHWS (m ODN)	R_2 (m)	Dune Toe Elevation (m ODN)
Southern Coast						
Seaton	2.23	167	0.09	2.35	1.55	3.9
Milendreath	2.32	162	0.10	2.35	1.71	4.1
Par Sands	1.39	138	0.03	2.05	0.65	2.7
Pentewan	1.67	97	0.11	2.35	1.15	3.5
Caerhays	2.21	141	0.08	2.49	1.10	3.6
Pendower	1.96	123	0.06	2.49	0.99	3.5
Swanpool	1.42	92	0.02	2.49	0.49	3.0
Maenporth	1.56	84	0.03	2.49	0.49	3.0
Kennack Sands	1.88	159	0.08	2.40	1.46	3.9
Poldhu Cove	3.91	266	0.04	2.40	1.69	4.1
Church Cove	3.50	242	0.05	2.40	1.76	4.2
Praa Sands	2.67	226	0.10	2.51	2.11	4.6
Marazion	2.31	166	0.01	2.55	0.84	3.4
Northern Coast						
Sennen Cove	4.87	308	0.09	2.55	3.12	5.7
Porthmeor	3.50	312	0.11	3.20	3.01	6.2
Lelant Towans	2.12	252	0.08	3.20	1.77	5.0
Harveys Towans[1]	2.65	314	0.03	3.20	1.80	5.0
Mexico Towans	2.64	313	0.05	3.20	1.88	5.1
Gwithian Towans	3.77	328	0.03	3.20	1.51	4.7
Porthtowan	3.61	295	0.04	3.20	1.76	5.0
Perranporth	3.76	294	0.02	3.40	1.43	4.8
Penhale	4.18	298	0.04	3.30	2.00	5.3
Holywell	4.04	290	0.08	3.30	2.43	5.7
Crantock	3.59	293	0.04	3.40	1.54	4.9
Fistral Beach	4.10	299	0.07	3.40	2.43	5.8
Porth	2.73	286	0.03	3.40	1.20	4.6
Mawgan Porth	3.34	294	0.03	3.50	1.47	5.0
Porthcothan	4.08	295	0.02	3.40	1.49	4.9
Treyarnon Bay	4.26	298	0.03	3.40	1.53	4.9
Constantine Bay	4.28	297	0.06	3.40	2.43	5.8
Harlyn	2.93	285	0.04	3.50	1.82	5.3
Trevone	3.10	287	0.03	3.50	1.33	4.8
Hawkers Cove	1.10	124	0.05	3.50	0.82	4.3
Rock Dune	1.99	287	0.09	3.50	1.75	5.2
Daymer Bay	2.24	285	0.06	3.50	1.68	5.2
Polzeath	3.12	278	0.02	3.50	1.27	4.8
Crackington Haven	3.84	276	0.09	3.50	2.89	6.4
Widemouth Bay	3.61	281	0.06	3.50	2.16	5.7
Summerleaze	3.01	277	0.03	3.50	1.37	4.9
Crooklets	3.40	284	0.07	3.50	2.05	5.5

[1] This site dune toe elevation was modified to equal that of the neighbouring site (Lelant Towans: 5.0 m ODN) as observations showed the predicted toe to be picking up a berm feature.

2.1.2. Dune Volume Change (δQ)

Changes in the dune volume between the first and each subsequent LiDAR survey (δQ) were calculated by integrating elevation changes above the dune toe within the mobile zone (defined in Section 2.1.2, examples shown in Figure 1-2). Following Wiggins et al. (2019), linear error theory was used to account for the vertical inaccuracy of the LiDAR data ($\delta Z \approx 0.15$ m) which propagates into the elevation change results when comparing two LiDAR-derived DEMs ($\sqrt{{\delta Z_{DEM1}}^2 + {\delta Z_{DEM2}}^2} = 0.21\ m$). The resultant propagated uncertainty (0.21 m) was used as a limit of detection – LiDAR spatial grid cells with elevation changes less than 0.21 m were excluded from the calculation of volume change as the change is below the detectable threshold.

At each dune site, δQ was averaged along the length of the dune system to obtain a volumetric change per meter of dune length (m^3/m). The error associated with δQ was determined by summing the vertical inaccuracies for each DEM over the cells utilized in the volume calculation, which included those above the dune toe and cells greater than the limit of detection. This error was then propagated between the two LiDAR-derived DEMs as $\sqrt{\sum \delta Z_{DEM1}(i_1)^2 + \sum \delta Z_{DEM2}(i_2)^2}$, where i_1 and i_2 are the indices of cells utilized in the volume calculation, and then averaged along the length of the dune. This represents a conservative estimate of the uncertainties in the calculation of dune volumetric change.

Linear regression fitted to the δQ timeseries was then used to explore any temporal trends in dune volume. As with δX, trends in dune volume with p-values < 0.05 were considered statistically significant. Figure 2-3 shows an example of δQ over time for Par Sands, where there is a statistically significant trend in δQ, showing a progressive increase in dune volume. The results for all sites are presented in Section 3.1.1.

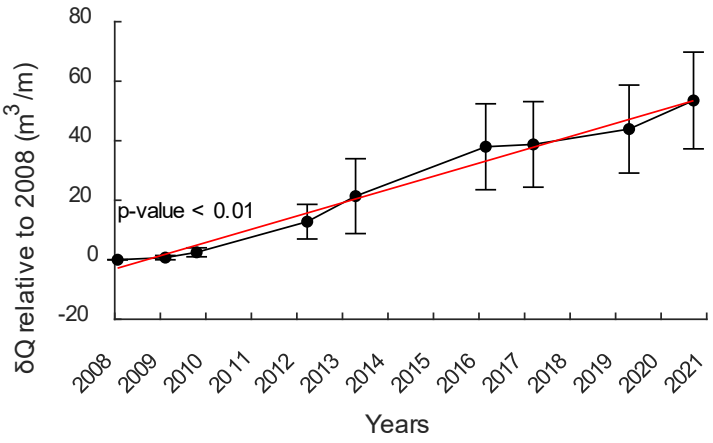


Figure 2-3. Change in dune volume (δQ) relative to the first (here 2008) LiDAR survey at Par Sands (black dots). Error bars show the LiDAR measurement error and the regression line describing the dune toe trend is shown in red.

2.2. Projections of Future Change

Future dune toe position and dune recession rates were estimated using two methods: (i) by extrapolating the observed dune toe changes, and (ii) using the Bruun rule. This approach accounts for the effects of sea-level rise (SLR) on the beach profile and therefore requires this information as input. The relative sea-level rise projections used in this investigation were based on the UK Climate Projections 2018 (UKCP18) (Palmer et al., 2018) obtained from the Met Office and account for sea-level rise and land subsidence or uplift. The key findings of the UKCP18 projections are:

- Sea level is projected to rise for all emission scenarios and at all locations around the UK.
- Changes in extreme water levels (e.g., surge and large tides) are mostly driven by changes in mean sea level.
- Sea level will continue to rise beyond the year 2100.
- There may be changes in the tidal characteristics and waves.
- Extreme wave heights may change on the order of 10 – 20% (although poor agreement between different model projections).

The key message from UKCP18 is that changes in mean sea level will have a significant influence on future extreme sea levels during storm events, and therefore coastal change (Palmer *et al.*, 2018). SLR predictions obtained at the closest output point for each dune site are similar. SLR estimates by 2100 corresponding to the high emission 50%ile along the Cornish coastline range between 0.79 and 0.82 m. An example for Seaton is provided in Figure 2-4.

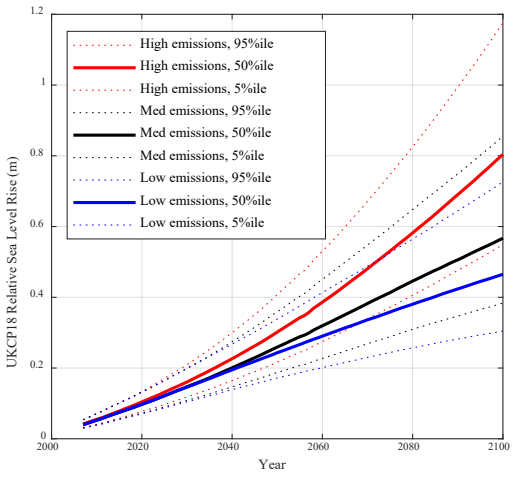


Figure 2-4. UKCP18 predictions of relative sea-level rise (SLR) at Seaton under high, medium, and low emissions scenarios (from https://ukclimateprojections-ui.metoffice.gov.uk/). Lower (5th percentile), median (50th percentile), and upper (95th percentile) predictions are also shown for each scenario, indicating the magnitude of uncertainty, determined from an ensemble of UKCP18 model predictions.

2.2.1. Future Projections Using Contemporary Trends

Dune retreat rates were projected into the future by extrapolating the rate of change in dune toe position obtained from the linear regression ($\delta X/\delta T$). Results obtained as the difference between the last and first survey ($\delta X_{last\text{-}first}/\delta T$) are also included. All results are presented Section 3.2.

2.2.2. Bruun Rule Projections

The Bruun rule (Bruun, 1954) is an equilibrium-based approach that allows us to model past and future beach evolution in response to SLR based on the idea that the shape of the beach profile is in equilibrium with the prevailing hydrodynamic (forcing) conditions and will thus maintain its shape as sea level rises. It therefore implies a landward and upward shift of the shoreline in response driven by SLR (Figure 2-5). The method has been used widely since the concept was proposed more than half a century ago but has been heavily critiqued in recent years for its over-simplification of coastal response (Cooper et al., 2020) as it carries a number of assumptions and limitations (Section 2.2.4). However, for the present study it provides a first-stage method for predicting future dune evolution, which will be improved upon with more complex models during later stages of the MS4S project. Bruun rule estimates of dune retreat in response to SLR in this study were based on the 2020/19 LiDAR toe position, and were projected to the year 2100 using the relationship:

$$R = S\frac{W_*}{h_* + B}$$

Where R is the shoreline retreat, S is the amount of sea-level rise over the forecast period, W_* is the width of the active shoreface, h_* is the morphological Depth of Closure (DoC) and B is the berm height (see Figure 2-5 for schematic). The latter includes the height of any dunes present (Rosati, 2013).

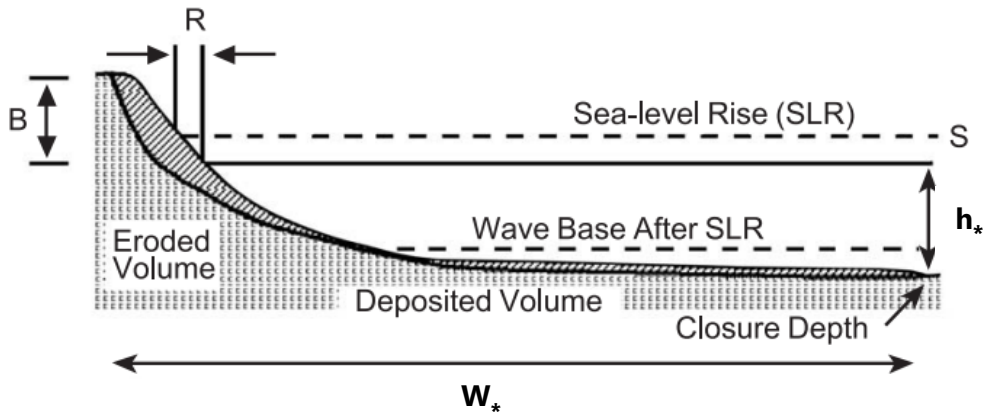


Figure 2-5. Schematic of Bruun rule showing current equilibrium beach profile and future profile due to sea level rise (from Cooper & Pilkey, 2004). Where *B* is the berm height, W_* is the width of active shoreface, and h_* is the morphological depth of closure.

The DoC is the water depth beyond which changes in the seabed morphology are assumed to approach zero. Three empirical equations (Birkemeier et al., 1985; Capobianco et al., 1997; Hallermeier, 1980) were used to calculate the DoC at each site, and the final DoC value for each dune site was defined as the average of the three estimates. The three empirical equations used are:

$DoC = 1.75H_e - \frac{57.9{H_e}^2}{g{T_e}^2}$ (Birkemeier et al., 1985),

$DoC = 2.28H_e - \frac{68.5{H_e}^2}{g{T_e}^2}$ (Hallermeier, 1980),

$DoC = k{H_{12hr}}^{0.67}$ (Capobianco et al., 1997).

Where H_e and H_{12hr} are calculated from wave heights shoaled (or reverse shoaled) from the model node depth to 20 m depth. H_e is the 'effective wave height', or significant wave height that is only exceeded 12 hours per year (i.e., with a probability of yearly exceedance of 0.137%), T_e is the associated wave period, and g is the acceleration due to gravity (Birkemeier et al., 1985, Hallermeier, 1980, Nicholls et al., 1996). H_{12hr} is the mean wave height over the 12-hour exceedance level, and k is a constant, here set to 3.4 following Nicholls et al. (1996).

The horizontal location of the DoC was determined at each 10-m spaced profile by interpolating bathymetric data from the SWCMP. The berm height (B) was taken as the maximum elevation within the 'Mobile Zone' for each profile (analogous to the dune crest in most cases). To account for longshore variability, a normal distribution was fitted to the longshore values of W_* and $(h_* + B)$ at each site. Figure 2-6 shows an example of such distribution for W_* and $(h_* + B)$ at Par Sands.

Using a normal distribution of W_* and $(h_* + B)$ and the distribution of S based on the UKCP18 predictions, a probabilistic Bruun rule approach using Monte Carlo sampling was applied, allowing for a distribution of retreat rates based on the longshore variability and uncertainty in SLR rates. From the normal distributions of W_*, $(h_* + B)$ and S, 10,000 values of each variable were randomly sampled and applied to the Bruun rule equation to predict the distribution of possible future dune toe retreat (R) with SLR. From the 10,000 predicted values of R, the 50th percentile value (the median value) was used as the predicted future retreat rate, with the 5th and 95th percentile values providing lower and upper confidence bounds, respectively. Results obtained using the Bruun are presented in Section 3.2 while the values of DoC elevation, the longshore median berm height elevation (B), the median width, and height of the shoreface $(h_* + B)$ used are included in Table 2-2.

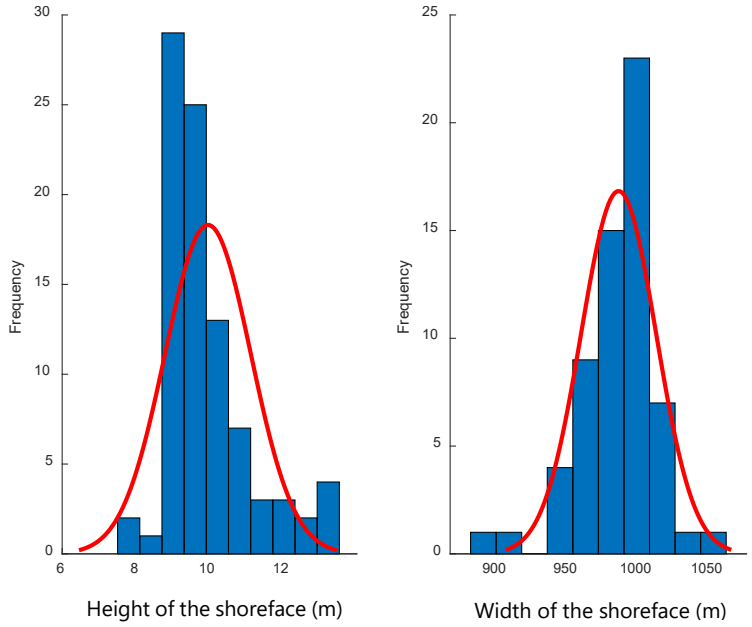


Figure 2-6. Example of longshore distribution of the height of the shoreface ($h_* + B$) (left) and width of the shoreface (W_*) (right) at Par Sands.

Table 2-2. Parameters used for the Bruun rule projections, including depth of closure (m ODN), median berm height, longshore median shoreface and longshore median height of the shoreface.

Site Name	Depth of Closure (m ODN)	Longshore median berm height in 2019/20 (m ODN)	Longshore median width of the shoreface (W_*) (m)	Longshore median height of the shoreface ($h_* + B$) (m)
Southern Coast				
Seaton	-6.16	3.43	417	9.86
Milendreath	-6.56	4.11	395	10.81
Par Sands	-4.79	4.77	984	9.94
Pentewan	-5.18	5.89	328	10.72
Caerhays	-5.43	4.08	487	9.96
Pendower	-5.21	4.58	332	9.90
Swanpool	-4.4	4.39	259	8.80
Maenporth	-4.77	4.79	523	9.52
Kennack Sands	-5.77	5.07	274	11.67
Poldhu Cove	-8.91	5.50	588	14.98
Church Cove	-8.58	6.73	559	15.46
Praa Sands	-6.77	6.25	321	16.05
Marazion	-5.97	4.98	586	11.33
Northern Coast				
Sennen Cove	-10.8	8.99	610	21.64
Porthmeor	-9.11	5.98	564	15.19
Lelant Towans	-7.52	8.51	854	15.92
Harveys Towans	-7.26	13.11	1126	21.01
Mexico Towans	-7.26	20.30	586	27.88
Gwithian Towans	-9.13	9.17	742	19.52
Porthtowan	-8.9	8.13	692	17.94
Perranporth	-9.18	14.33	965	23.44
Penhale	-9.68	15.05	770	26.58
Holywell	-9.77	12.85	658	23.34
Crantock	-9.87	20.40	1044	28.13
Fistral Beach	-9.87	13.41	750	21.36
Porth	-8.34	5.24	1049	13.60
Mawgan Porth	-8.69	6.74	977	15.34
Porthcothan	-14.11	9.06	1157	23.42
Treyarnon Bay	-10	5.98	934	16.51
Constantine Bay	-10.07	13.32	868	22.13
Harlyn	-8.47	7.73	547	16.27
Trevone	-8.47	5.33	597	13.68
Hawkers Cove	-7.05	9.16	1498	15.98
Rock Dune	-5.50[2]	17.20	567	22.53
Daymer Bay	-5.50[2]	6.16	605	13.19
Polzeath	-8.35	5.04	1051	13.99
Crackington Haven	-9.29	6.41	708	15.84
Widemouth Bay	-9.04	9.91	800	19.08
Summerleaze	-9.39	11.37	960	21.24
Crooklets	-8.69	6.62	769	15.15

[2] These sites DoC were modified to -5.5 m ODN as these sites are within an estuary and the profile depth does not reach the DoC calculated empirically.

2.2.3. Contemporary Bruun Rule Predictions

The Bruun rule can be applied to contemporary/historic data to estimate the amount of coastal recession that is expected to have occurred due to sea level rise in the past. For this, the Bruun rule approach, detailed above, was applied to historic sea levels, substituting UKCP18 SLR predictions with rates of SLR observed at Newlyn (from Data at PSMSL) over the survey period (4.9 mm/yr) to obtain estimates of retreat rates due to SLR over the past 15 years. These results are presented in Section 3.1.2. along with two methods of estimated observed rates of change in dune toe position.

2.2.4. Assumptions and Limitations

The projections presented in Section 3.2. are simple parametric predictions of dune evolution using the Bruun rule or extrapolated from observed contemporary rates of change. These approaches are simplistic and carry a number of assumptions and limitations, and therefore have a high degree of uncertainty.

The Bruun rule approach assumes the profile shape will be translated upwards and landwards through SLR-driven migration of the beach. This approach includes the following limitations:

- Unlimited sediment supply is assumed, and no account is taken of the depth of sediment over the underlying bedrock.
- Local sources and sinks of sediment are ignored.
- Input and output of sediment from longshore transport is not considered.
- Additional sediment transport processes, in particular onshore transport (aeolian transport, overwash), are disregarded.
- Other potential responses to SLR are ignored, for example, where sediment is abundant in the nearshore sites have been shown to accrete/ advance due to SLR (Brooke et al., 2019, Thom, 1984).
- Does not consider the rate of change of SLR.
- The geological material or topography of the area of projected retreat is disregarded (Cooper et al., 2020), including the sediment supply from eroding dunes.
- Does not account for structures (e.g., rock armour) present at some dunes sites.

For the contemporary rates of change, the primary assumption is that the observed trends are representative over a multi-decadal timescale and will continue unchanged into the future.

3. Results

3.1. Contemporary Dune Evolution

3.1.1. Temporal trends of dune morphology

Analysis of the LiDAR data revealed great variability in the changes in dune toe position (Figure 3-1) and sediment volume (Figure 3-2) over the survey period across the 40 sites. In real terms, dune toe position changed at rates (Table 3-2) ranging from 2.3 m of retreat per year (Crantock Beach), to 2 m of advance per year (Hawkers Cove), with net changes ranging from 46.7 m of retreat (Rock dune) to 20.2 m of advance (Hawkers Cove) over the survey period. Dune volume changes were similarly variable across Cornwall, with rates (Table 3-2) ranging from 11.45 m^3/m of sediment loss per year (Crantock Beach), to 4.3 m^3/m of sediment gain per year (Summerleaze), with net changes ranging from 145.7 m^3/m of sediment lost (Crantock Beach) to 58.4 m^3/m of sediment gained (Summerleaze) over the survey period.

The winter of 2013-14 was exceptionally energetic (Masselink et al., 2016) and caused widespread coastal erosion and flooding, which can be seen in some of the 40 sites as a sharp change in volume (Figure 3-2), with the majority of impacted sites located on the northern coast (Sennen Cove, Porthmeor, Mexico Towans, Perranporth, Penhale, Holywell, Fistral Beach, Mawgan Porth, Porthcothan, Constantine Bay, Harlyn, Daymer Bay). However, large volume losses were also observed over other periods at other locations (Figure 3-1 and Figure 3-2). For example, at Lelant Towans greater volume loss is observed between September 2009 –March 2011, and between Feb 2016 – April 2017, than was seen during the 2013-14 winter, and Rock Dunes experienced significant volume loss between April 2019 – November 2020. In addition, Crantock experienced greater volume loss between March 2017 – April 2019, than over the 2013-14 winter, which has been attributed to a shift in the location of the main river channel that exits through the beach (Hird, 2021).

To benchmark our analysis, we compared our results with the study conducted by Burvingt and Castelle (2023), which assessed dune changes following the 2013/14 storms at Penhale and Mexico Towans (where they refer to Mexico Towans as Gwithian). They estimate similar retreat of the dune toe following the winter of 2013–14 of around 17 m at Penhale (compared to our estimate of 16.8 m) and 8–10 m at Mexico Towans (compared to our estimate of 8.8 m) and observed similar recovery patterns. Estimates of δQ are not comparable between the studies because the volume changes are calculated over different defined areas.

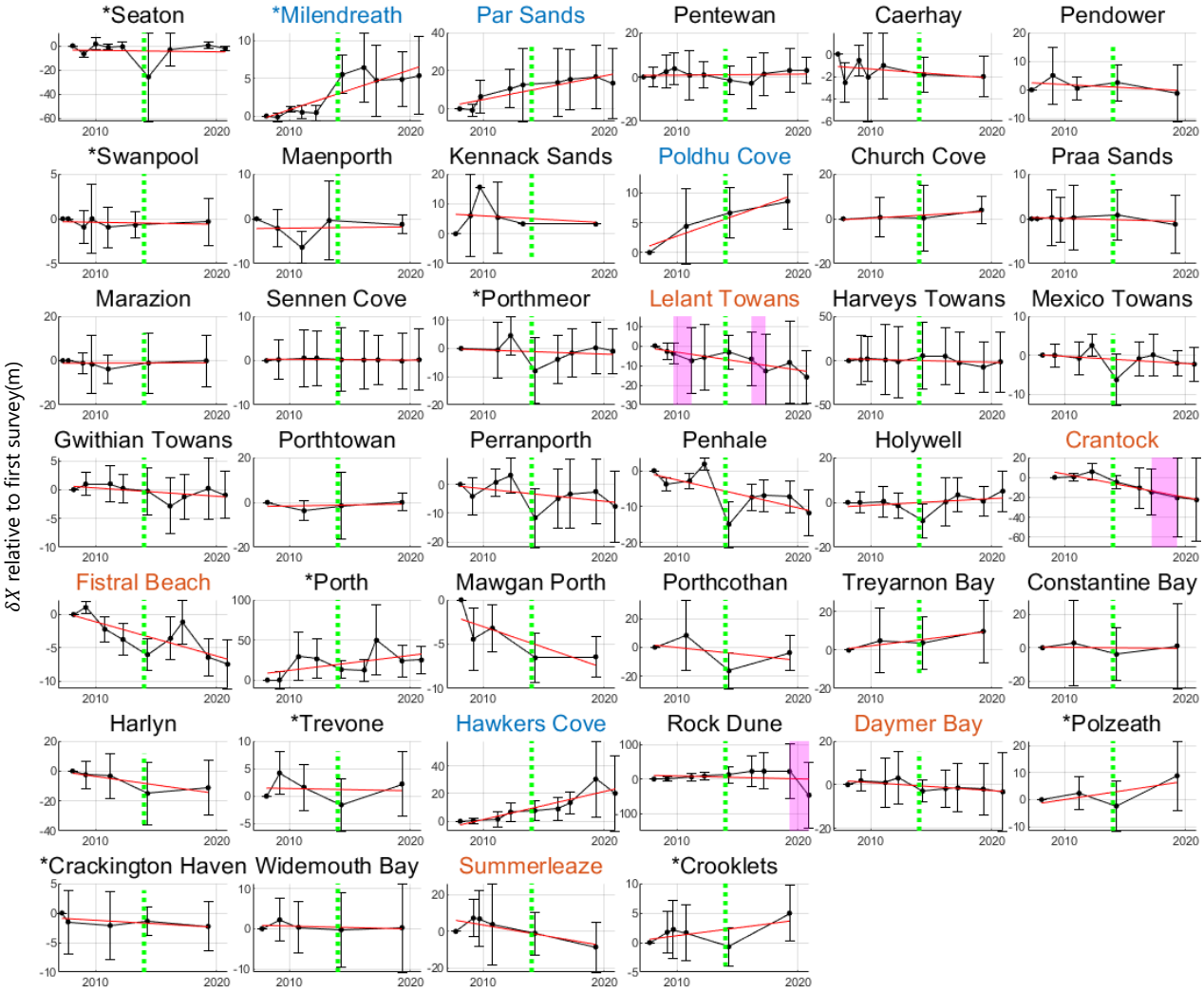


Figure 3-1. Time series of dune toe migration relative to the first LiDAR survey (δX) for the 40 sites (black dots). A negative change represents retreat, and a positive change represents advance. Black error bars show the longshore standard deviation, and the red line is the linear fit (trend line). Site names with a statistically significant trend (p-values < 0.05) are displayed in orange for retreating sites and blue for advancing sites. * indicates sites without dunes. The green dashed lines mark the winter of 2013/14, the most energetic winter in at least 65 years (Masselink et al., 2016). Magenta shading show periods over which significant volume changes have occurred at Lelant Towams, Crantock and Rock Dune discussed in this section.

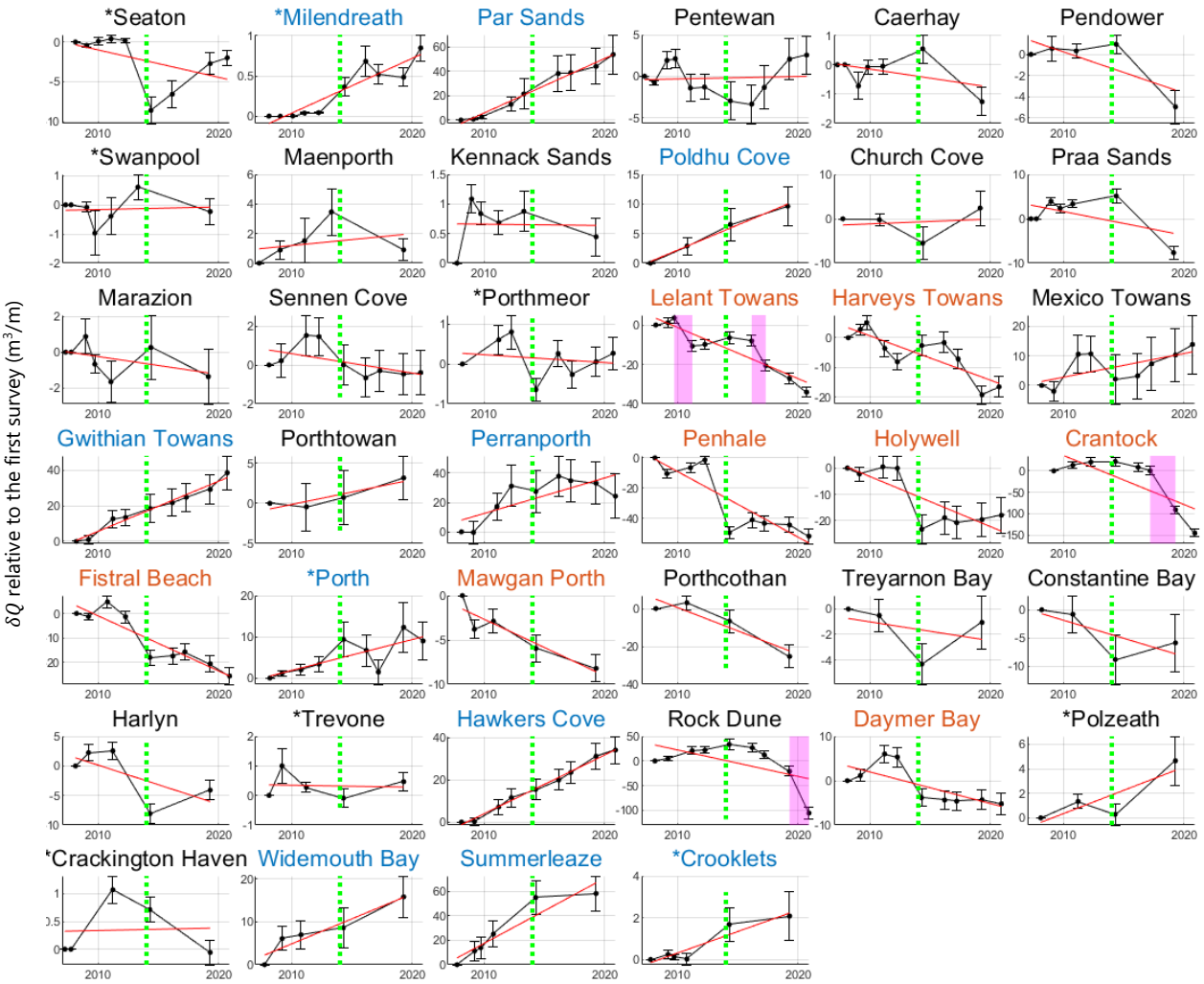


Figure 3-2. Time series of dune volume change (m³/m) relative to the first LiDAR survey (δQ) for the 40 sites (black dots). A negative change represents volume loss and a positive change volume gain. Black error bars show the LiDAR measurement error, and the red line is the linear fit (trend line). Site names with a statistically significant trend (p-values < 0.05) are displayed in orange for eroding sites and blue for accreting sites. * indicates sites without dunes. The green dashed lines show the winter of 2013/14, the most energetic winter in at least 65 years (Masselink et al., 2016)). Magenta shading show periods over which significant volume changes have occurred at Lelant Towams, Crantock and Rock Dune discussed in this section.

Figure 3-4 and Table 3-1 show the net change in δQ and δX between the first and last LiDAR data represented spatially for the 40 dune sites studied across Cornwall. Over this period, 19 sites (48%) gained sediment and 21 (53%) sites lost sediment, while in terms of dune toe position, 17 sites (43%) advanced, and 23 sites (58%) retreated. This indicates that some of the dunes that gained in volume over the survey period, also retreated landward. This could be due to dune roll-over, where sediment is transported from the front of the dune to the top and back of the dune during storm events (Davidson-Arnott, 2021). About half of the sites on the southern coast have retreated over the survey period (7 out of 13 sites; 54%), while most of the sites on the northern coast have retreated (16 out of 27 sites; 59%).

Looking more closely at the sediment gains vs losses at each of the dune sites (Figure 3-3), more than half the dunes show signs of rollover (where sediment is accreting on top of the dune), although in many cases this is outpaced by erosion of the dune front. For example, the dunes at Crantock have actually gained more than 25 m^3/m over the survey period (i.e., more than the total dune volume change seen at a number of other dunes), but these sediment gains are massively outpaced by the erosion of the dune front (>175 m^3/m of sediment lost). While sediment gains on top of the dune indicate that aeolian driven rollover is occurring in most cases, at some sites alongshore variability in dune response is seen, with sediment gains at one end of the dune frontage and losses at the other (Appendix D). For example, Daymer Bay, Harvey Towans, Holywell, Treyarnon, Constantine, Harlyn, Rock Dune, and Daymer Bay, are all gaining sediment at one end of the dune frontage (often near to a river outfall or estuary), while losing sediment along the remaining dune frontage.

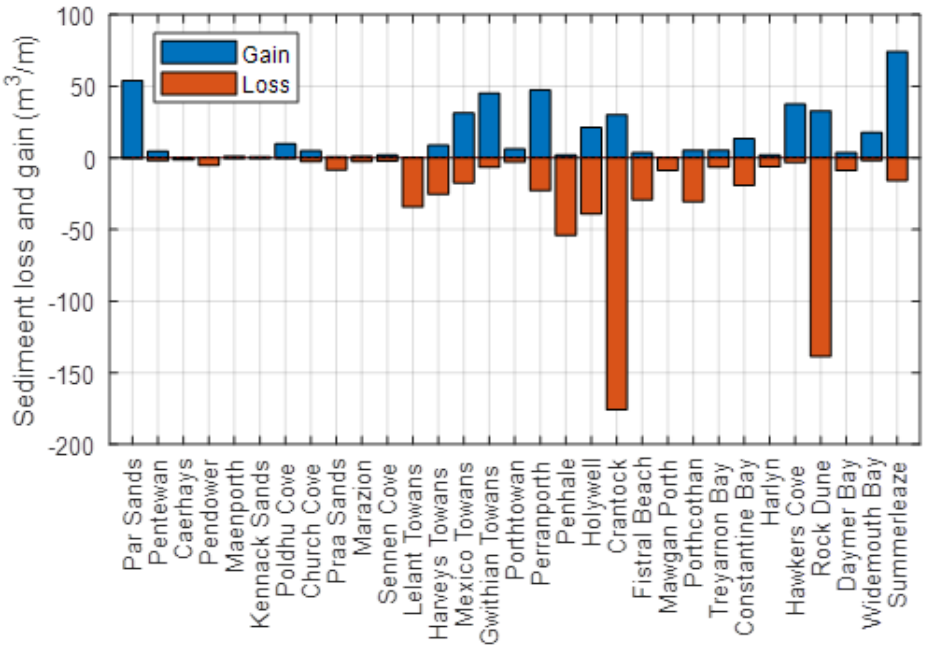


Figure 3-3. Sediment volume gains (blue) vs losses (red) for the 34 dune sites in the study region over the study period.

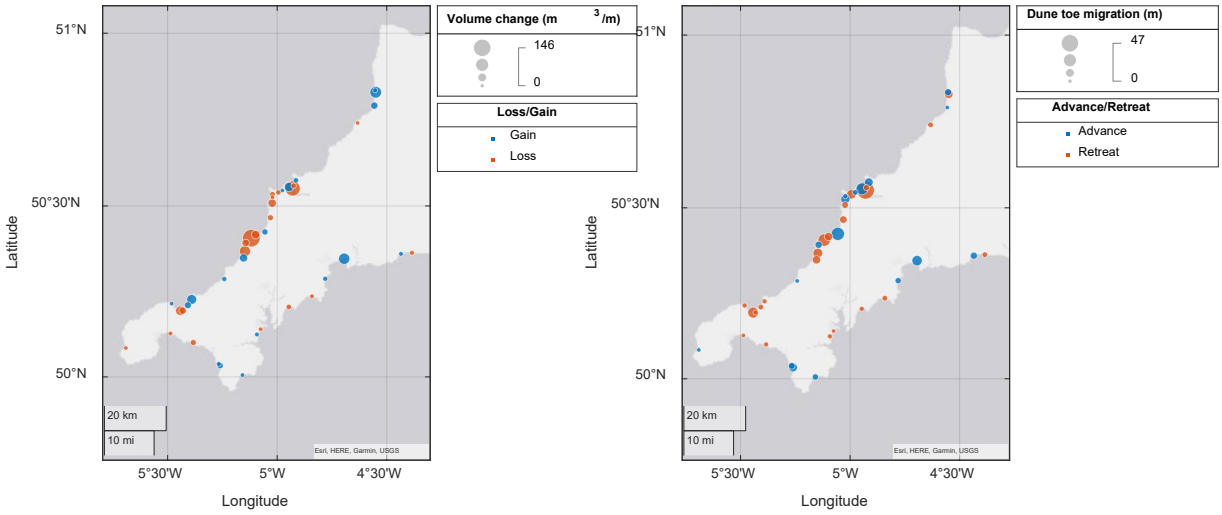


Figure 3-4. Spatial representation of dune changes observed over the LiDAR survey period for the 40 MS4S sites. Volume change per meter dune width above the dune toe (left); and dune toe migration (δX) (right). Volume loss and dune toe retreat are shown in orange and volume gain and dune toe advance are shown in blue. These results are presented analytically in Table 3-1.

For all sites, the relationship between the rate of dune volumetric change $\delta Q/\delta T$ and the rate of dune toe change $\delta X/\delta T$, both determined from the linear trend (regardless of significance), is shown in Figure 3-5. With all sites considered, there is a statistically significant correlation between $\delta Q/\delta T$ and $\delta X/\delta T$. In other words, dunes that lose sediment fastest tend to retreat landward fastest, and dunes that gain sediment fastest tend to prograde seaward fastest. However, most sites do not have a statistically significant trend in either δQ or δX, or both (detailed in Table 3-2).

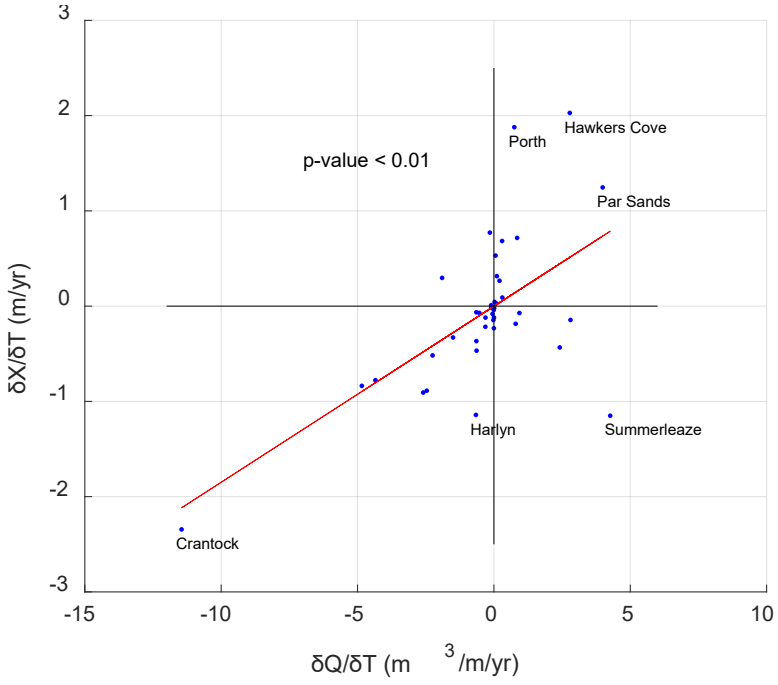


Figure 3-5. Relationship between the rate of dune volumetric change $\delta Q/\delta T$ and the rate of dune toe change $\delta X/\delta T$ for the 11/12-year monitoring period for all sites. Sites with absolute $\delta X/\delta T$ rates larger than 1m/yr are labelled

Figure 3-6 shows the relationship between $\delta Q/\delta T$ and $\delta X/\delta T$ for the subset of sites with statistically significant relationships of δQ and δX. These sites also exhibit a statistically significant correlation between $\delta Q/\delta T$ and $\delta X/\delta T$; and three distinct modes of dune response:

1) Some dunes gain volume and advance, which are likely dominated by aeolian (wind-driven) sediment transport from the beach into the dunes (n = 3)
2) Some dunes lose volume and retreat, which are likely dominated by storm erosion (n = 4)
3) Some dunes gain volume while retreating, referred to as roll-over, which are likely dominated by storm erosion of the frontal dune and aeolian sediment transported from the beach and the front of the dune to the top and back of the dune (n =1)

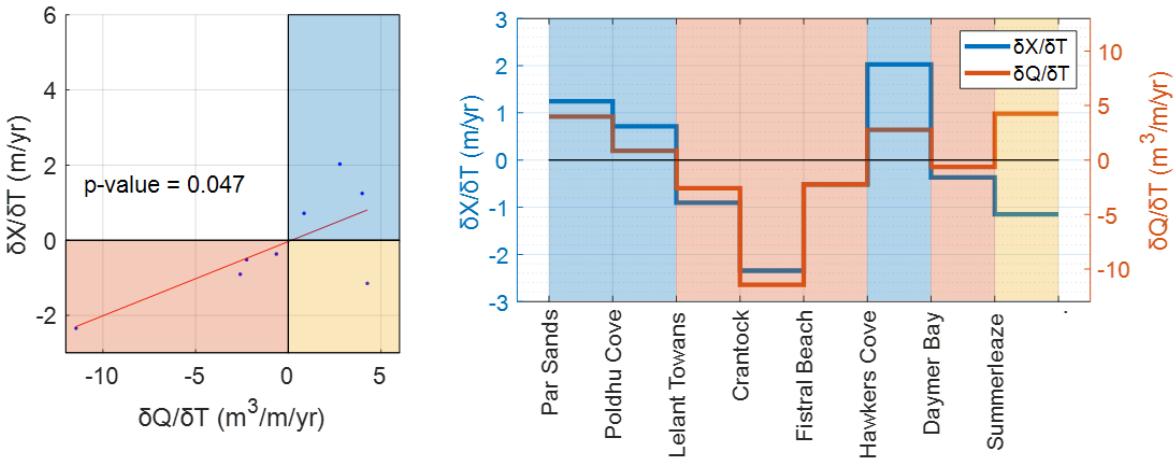


Figure 3-6. Relationship between the rate of dune volumetric change $\delta Q/\delta T$ and the rate of dune toe change $\delta X/\delta T$ (left) and the values of $\delta Q/\delta T$ and $\delta X/\delta T$ for each site (right) over the survey period. Only sites with a statistically significant trend in volume and toe position were included. Highlighted in blue are sites that are gaining sediment and advancing, in orange are sites that are losing sediment and retreating, and in yellow the one site that is gaining sediment and retreating.

Table 3-1. Net volume change per meter dune width above the dune toe ($\delta Q_{last-first}$) and net dune toe migration ($\delta X_{last-first}$) observed over the LiDAR survey period.

Site Name		Dune/Not Dune	$\delta X_{last-first}$ (m)	$\delta Q_{last-first}$ (m^3/m)
Southern Coast				
Seaton		Not Dune	-2.2	-2.0
Milendreath		Not Dune	5.3	0.8
Par Sands		Dune	13.5	53.5
Pentewan		Dune	2.9	2.5
Caerhays		Dune	-2.0	-1.3
Pendower		Dune	-1.2	-5.0
Swanpool		Not Dune	-0.3	-0.2
Maenporth		Dune	-1.3	0.9
Kennack Sands		Dune	3.2	0.4
Poldhu Cove		Dune	8.6	9.6
Church Cove		Dune	3.9	2.4
Praa Sands		Dune	-1.2	-7.6
Marazion		Dune	-0.1	-1.4
Northern Coast				
Sennen Cove		Dune	0.2	-0.4
Porthmeor		Not Dune	-1.0	0.3
Lelant Towans		Dune	-15.9	-34.0
Harveys Towans		Dune	-1.3	-16.6
Mexico Towans		Dune	-2.3	13.8
Gwithian Towans		Dune	-1.0	38.5
Porthtowan		Dune	0.0	3.2
Perranporth		Dune	-7.6	24.3
Penhale		Dune	-11.8	-51.9
Holywell		Dune	5.0	-17.9
Crantock		Dune	-22.4	-145.7
Fistral Beach		Dune	-7.5	-25.5
Porth		Not Dune	24.9	9.0
Mawgan Porth		Dune	-6.4	-8.2
Porthcothan		Dune	-3.8	-25.3
Treyarnon Bay		Dune	9.9	-1.1
Constantine Bay		Dune	1.1	-5.9
Harlyn		Dune	-11.2	-4.1
Trevone		Dune	2.2	0.5
Hawkers Cove		Dune	20.2	34.2
Rock Dune		Dune	-46.7	-105.7
Daymer Bay		Dune	-3.3	-5.2
Polzeath		Not Dune	8.9	4.7
Crackington Haven		Not Dune	-2.3	-0.1
Widemouth Bay		Dune	0.2	15.9
Summerleaze		Dune	-8.6	58.4
Crooklets		Not Dune	5.0	2.1

Table 3-2. Rates of change derived from linear regression ($\delta X/\delta T$; $\delta Q/\delta T$) and associated p-values for all sites. Negative trends signify retreat of the dune toe ($\delta X/\delta T$) and loss of dune volume ($\delta Q/\delta T$) respectively appear in red. Statistically significant ($p < 0.05$) trends, wither positive or negative, are highlighted in bold font.

Site Name	Dune/Not Dune	$\delta X/\delta T$ (m/yr)	p-value	$\delta Q/\delta T$ ($m^3/m/yr$)	p-value
Southern Coast					
Seaton	Not Dune	-0.12	0.87	-0.31	0.20
Milendreath	Not Dune	**0.53**	**0.00**	**0.06**	**0.00**
Par Sands	Dune	**1.25**	**0.00**	**3.99**	**0.00**
Pentewan	Dune	0.04	0.77	0.03	0.85
Caerhays	Dune	-0.08	0.41	-0.05	0.31
Pendower	Dune	-0.22	0.48	-0.31	0.14
Swanpool	Not Dune	-0.02	0.65	0.01	0.87
Maenporth	Dune	0.03	0.93	0.08	0.64
Kennack Sands	Dune	-0.23	0.73	0.00	0.96
Poldhu Cove	Dune	**0.72**	**0.04**	**0.85**	**0.01**
Church Cove	Dune	0.31	0.14	0.11	0.84
Praa Sands	Dune	-0.07	0.27	-0.54	0.22
Marazion	Dune	0.01	0.95	-0.10	0.29
Northern Coast					
Sennen Cove	Dune	-0.02	0.40	-0.10	0.12
Porthmeor	Not Dune	-0.15	0.68	-0.02	0.67
Lelant Towans	Dune	**-0.91**	**<0.01**	**-2.59**	**<0.00**
Harveys Towans	Dune	-0.33	0.27	**-1.50**	**<0.00**
Mexico Towans	Dune	-0.19	0.37	0.80	0.07
Gwithian Towans	Dune	-0.15	0.14	**2.81**	**<0.01**
Porthtowan	Dune	0.09	0.76	0.31	0.09
Perranporth	Dune	-0.43	0.24	**2.42**	**0.02**
Penhale	Dune	-0.78	0.06	**-4.34**	**<0.01**
Holywell	Dune	0.30	0.34	**-1.90**	**0.01**
Crantock	Dune	**-2.34**	**<0.01**	**-11.45**	**0.03**
Fistral Beach	Dune	**-0.52**	**0.01**	**-2.25**	**0.00**
Porth	Not Dune	1.88	0.13	**0.75**	**0.02**
Mawgan Porth	Dune	-0.47	0.12	**-0.64**	**0.02**
Porthcothan	Dune	-0.89	0.58	-2.46	0.07
Treyarnon Bay	Dune	0.77	0.09	-0.15	0.63
Constantine Bay	Dune	-0.07	0.89	-0.64	0.27
Harlyn	Dune	-1.14	0.10	-0.66	0.23
Trevone	Dune	-0.04	0.89	-0.01	0.91
Hawkers Cove	Dune	**2.03**	**<0.01**	**2.78**	**<0.01**
Rock Dune	Dune	-0.84	0.66	-4.84	0.12
Daymer Bay	Dune	**-0.37**	**0.02**	**-0.64**	**0.03**
Polzeath	Not Dune	0.68	0.33	0.30	0.15
Crackington Haven	Not Dune	-0.12	0.22	0.00	0.94
Widemouth Bay	Dune	-0.07	0.57	0.94	**0.01**
Summerleaze	Dune	**-1.15**	**0.05**	**4.26**	**0.01**
Crooklets	Not Dune	0.27	0.24	**0.21**	**0.01**

3.1.2. Comparison of contemporary rates of dune toe change

Figure 3-7 and Table 3-3 show the observed rates of dune toe change calculated from the gradient of the linear trend line ($\delta X/\delta T$) and the change in dune toe from the first to last survey ($\delta X_{last\text{-}first}/\delta T$), as well as the estimated Bruun retreat rates for the past 15 years based on SLR observed at Newlyn (referred to as hindcasting). The two methods of calculating contemporary rates of dune toe change mostly agree on whether the system is retreating or advancing. Rock Dune has the largest disparity between the two methods as the site experienced a retreat of ~80 m between 2019 and 2020, prior to which the dune toe was advancing.

Several sites that have been retreating over the past 12 years have retreat rates that far exceed the estimated Bruun retreat rates (Figure 3-7 and Table 3-3). This indicates that contemporary trends are mostly greater than estimated retreat due to SLR and therefore likely a result of other processes (i.e., storm erosion and/or estuarine or riverine influence). Sites with similar contemporary retreat rates to Bruun estimates include Widemouth Bay, Mexico Towans and Crackington Haven

The lack of correspondence between measured contemporary change in the dune toe position and that hindcasted using the Bruun rule for the majority of the dune sites raises the question as to what approach is most appropriate for forecasting future dune change and is addressed in the next section.

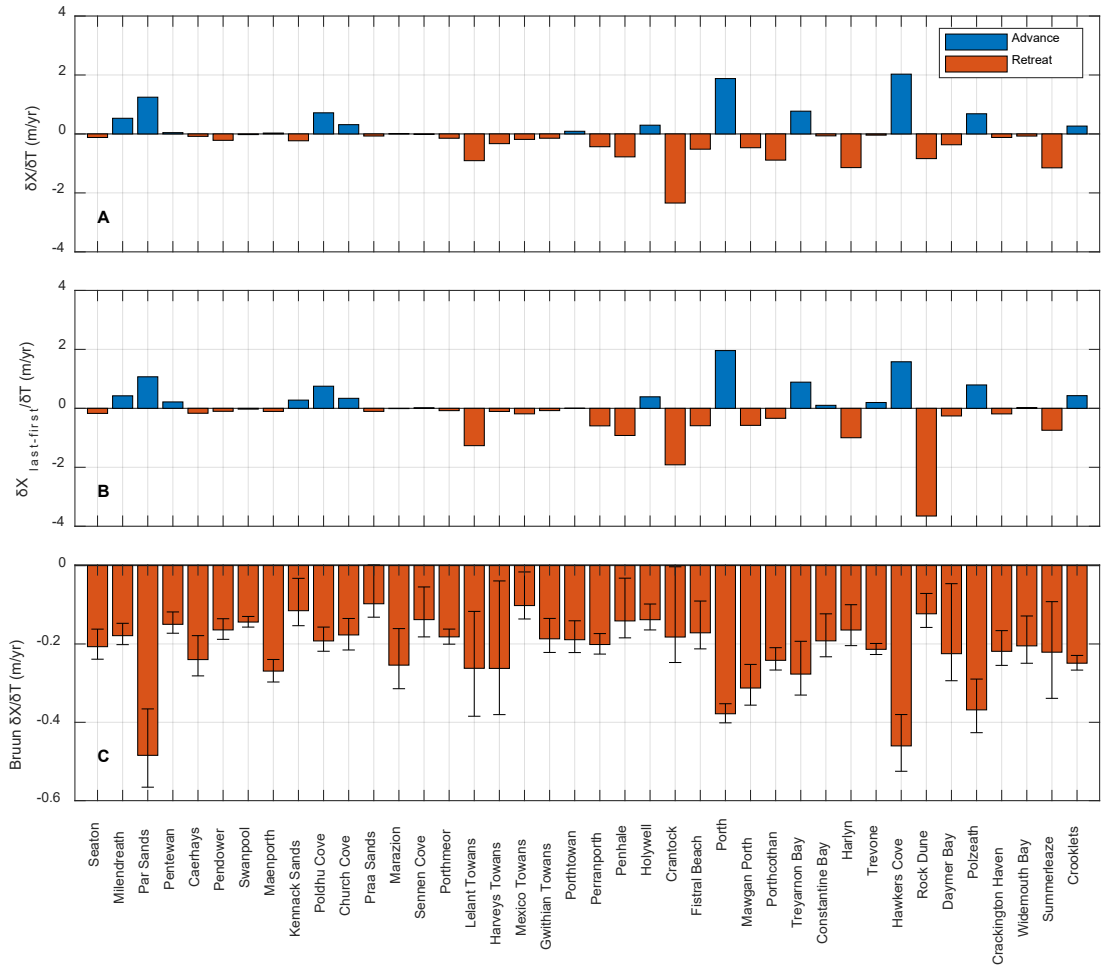


Figure 3-7. (A) Observed rates of dune toe change calculated from the gradient of the linear trend line ($\delta X/\delta T$), (B) from the change in dune toe from the first to last survey $\delta X_{last\text{-}first}/\delta T$, and (C) Bruun rule rates estimated for the past 15 years of SLR observed at Newlyn. Positive results indicate dune toe advance and negative results indicate dune toe retreat.

Table 3-3. Rates of dune toe change calculated from the gradient of the linear trend line $\delta X/\delta T$ and from δX calculated from the last survey $\delta X_{last\text{-}first}/\delta T$, as well as Bruun rule rates estimated for the past 15 years of SLR observed at Newlyn. Sites with statistically significant advancing trends are highlighted in blue and those with statistically significant retreating trends in red. Positive results indicate dune toe advance and negative results indicate dune toe retreat.

Site Name	$\delta X/\delta T$ – From linear trend (m/yr)	$\delta X_{last\text{-}first}/\delta T$ – From last survey (m/yr)	Estimated past Bruun retreat rate (m/yr)
Southern Coast			
Seaton	-0.12	-0.17	0.21
Milendreath	0.53	0.42	0.18
Par Sands	1.25	1.07	0.48
Pentewan	0.04	0.22	0.15
Caerhays	-0.08	-0.17	0.24
Pendower	-0.22	-0.10	0.16
Swanpool	-0.02	-0.03	0.14
Maenporth	0.03	-0.10	0.27
Kennack Sands	-0.23	0.28	0.12
Poldhu Cove	0.72	0.75	0.19
Church Cove	0.31	0.34	0.18
Praa Sands	-0.07	-0.10	0.10
Marazion	0.01	-0.01	0.25
Northern Coast			
Sennen Cove	-0.02	0.02	0.14
Porthmeor	-0.15	-0.08	0.18
Lelant Towans	-0.91	-1.27	0.26
Harveys Towans	-0.33	-0.11	0.26
Mexico Towans	-0.19	-0.19	0.10
Gwithian Towans	-0.15	-0.08	0.19
Porthtowan	0.09	0.00	0.19
Perranporth	-0.43	-0.59	0.20
Penhale	-0.78	-0.92	0.14
Holywell	0.30	0.39	0.14
Crantock	-2.34	-1.92	0.18
Fistral Beach	-0.52	-0.59	0.17
Porth	1.88	1.96	0.38
Mawgan Porth	-0.47	-0.58	0.31
Porthcothan	-0.89	-0.34	0.24
Treyarnon Bay	0.77	0.89	0.28
Constantine Bay	-0.07	0.10	0.19
Harlyn	-1.14	-1.00	0.16
Trevone	-0.04	0.20	0.21
Hawkers Cove	2.03	1.58	0.46
Rock Dune	-0.84	-3.65	0.12
Daymer Bay	-0.37	-0.26	0.22
Polzeath	0.68	0.79	0.37
Crackington Haven	-0.12	-0.19	0.22
Widemouth Bay	-0.07	0.02	0.20
Summerleaze	-1.15	-0.74	0.22
Crooklets	0.27	0.43	0.25

3.2. Projected Future Change

3.2.1. Future Projections Using Contemporary Trends

Dune retreat rates were projected into the future by extrapolating the contemporary rate of change in dune toe from the linear trend line ($\delta X/\delta T$) and change in dune toe from the first to last survey ($\delta X_{last\text{-}first}/\delta T$). These results are presented in Figure 3-8 and values presented in Appendix B. As discussed in Section 3.1.2 there are some disparities between $\delta X/\delta T$ and $\delta X_{last\text{-}first}/\delta T$ and subsequent extrapolated projections.

For Lelant Towans, Crantock, and Summerleaze (sites with statistically significant trend in δX), extrapolation of the $\delta X/\delta T$ trend to the year 2100 results in a forecasted retreat of > 100 m. Conversely, at Hawkers Cove, the dunes are predicted to advance seaward by > 100 m by the year 2100. The key assumption of the extrapolation approach is that the observed contemporary trends are representative over a multi-decadal timescale and will continue unchanged into the future; this is considered highly unlikely. For this reason, we consider the projections based on extrapolating the contemporary trends of interest, but not sufficiently robust to inform long-term management decisions.

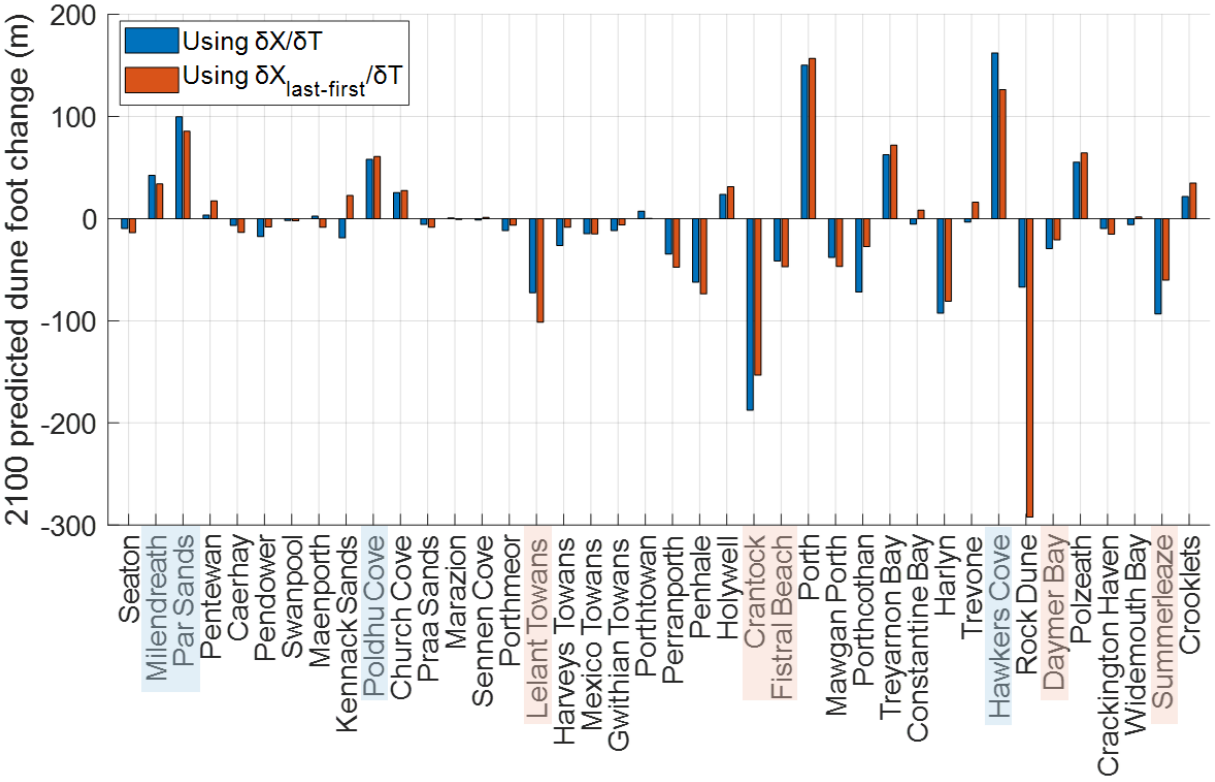


Figure 3-8. 2100 predicted retreat (m) for the 40 sites using observed rates of change based on two methods: (1) the gradient of the linear trend line ($\delta X/\delta T$); and (2) the change in dune toe from the first to last survey ($\delta X_{last\text{-}first}/\delta T$). Negative results are for dune toe retreat and positive trends are for dune toe advance. Sites names with significant trends are highlighted in red (for negative trends) and blue (for positive trends).

3.2.2. Future Bruun Rule Projections

Figure 3-9 shows projections of future dune toe change from 2019/20 to the year 2100 using the Bruun rule and Figure 3-10 summarises these results for the year 2100, both with confidence bounds from the probabilistic Bruun rule approach (see Section 2.2.1). Values of the 2100 retreat are presented in Appendix B, Table B-1. The Bruun dune toe projections over this time frame range from 13 m of retreat at Praa Sands (the steepest site) to 61 m of retreat at Par Sands (the most gently sloping site). Interestingly, the sites with the largest projected retreat are Par Sands, Hawkers Cove and Porth because they all have a gently sloping profile. However, all of these sites exhibit significant advancing trends suggesting the existence of a steady source of sediment over the survey period. Because the Bruun rule assumes a closed sediment budget, it is unsurprising that the predicted retreat is much larger than observed at these prograding sites. This underscores a limitation in the results obtained through the application of the Bruun rule, which is further discussed in Section 3.3. Despite these constraints, the estimates provided by the Bruun rule remain the best estimate of sea level induced dune changes available at this stage (i.e., ignoring sediment sources and sinks), not least because it remains uncertain to what extent the sediment source observed over the past decade will persist in the future and to what extent it will offset the effects of sea-level rise-induced retreat. Appendix C shows the Bruun rule results mapped for each site.

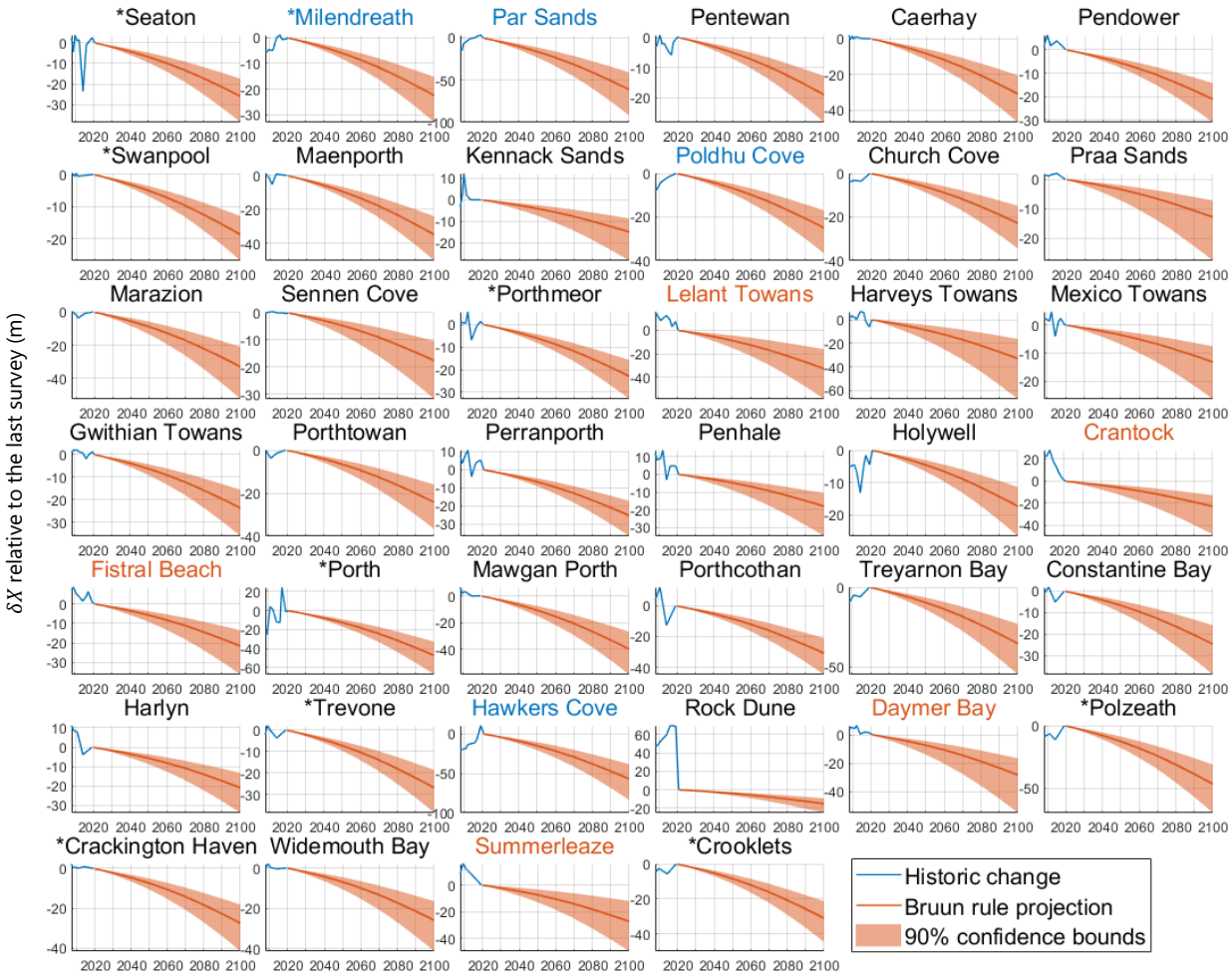


Figure 3-9. Contemporary dune toe change over the survey period (blue) and Bruun rule projected future change (orange) to the year 2100 relative to the last LiDAR survey for the 40 Cornish dune sites. Positive results indicate dune toe advance and negative results indicate dune toe retreat. Sites names with a statistically significant (p-values < 0.05) historic trend are displayed in orange for retreating sites and blue for advancing sites. * indicates sites without dunes.

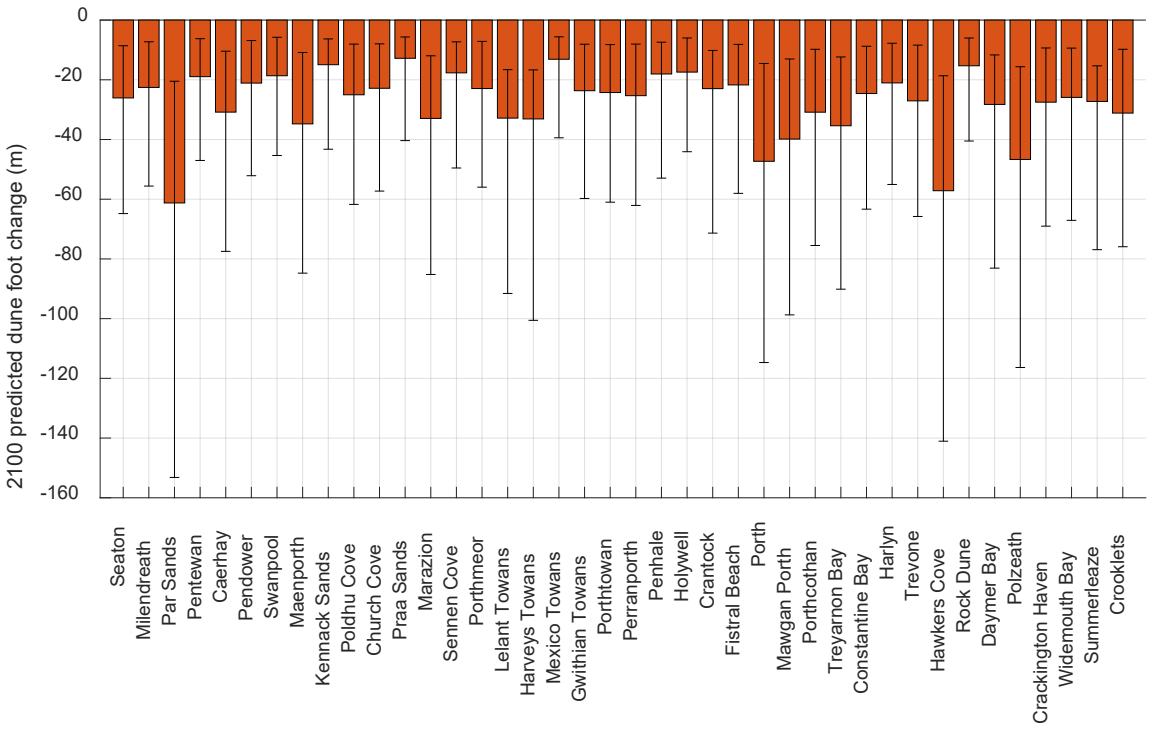


Figure 3-10. 2100 predicted retreat (m) for the 40 sites using the probabilistic Bruun rule approach (detailed in Section 2.2.2). Negative results indicate dune toe retreat. Red bars indicate median (50%) estimate, and the error bars represent 5th and 95th percentile values.

3.3. Caveats

As stated in Section 2.2.3 there are significant assumptions and limitations to the 'traditional' methods used in this study, which contribute a substantial amount of uncertainty to the results. While we have attempted to address some of the uncertainties within the inputs to the Bruun rule through the use of site-specific forcing factors and a probabilistic approach, the Bruun rule itself ignores a number of physical processes that are known to occur at the studied Cornish dune sites. These can be summarised as follows, and suggestions are made as to which processes may be addressed later in the MS4S project:

- **Underlying geology can limit dune retreat in the future.** Climbing dunes, such as at Crantock, and many other Cornish dune sites, will not continue to retreat at their contemporary rate indefinitely as the underlying bedrock will eventually be exposed, limiting further toe retreat. Quantifying the depth of sediment at key dune sites will therefore be important for the MS4S project to provide realistic predictions of future dune evolution, allowing the position of the bedrock to be accounted for.
- **Local sources and sinks of sediment may change in the future.** Dunes such as Rock Dune and Hawkers Cove that are located in estuaries are subject to drastic fluctuations in their sediment budget due to the dynamic nature of estuaries. Therefore, depending on the position of the river/estuarine channel and/or the estuarine supply of sediment, contemporary rates of dune growth

are unlikely to remain constant into the future. One example of this is Rock dune, which is a migrating spit/foreland, and the erosion on the updrift end is balanced by accretion at the downdrift end, making the observed retreat rates an unreliable predictor of future behaviour. Similarly, the dynamics of the dune systems flanking the Hayle estuary (Harveys and Mexico Towans) are likely to be significantly affected by estuarine mouth processes.

- **Bruun rule assumes there are no sediment inputs or outputs due to gradients in longshore transport.** Although this limitation has been addressed to some extent during the present study by considering contemporary rates of dune retreat, any changes in longshore sediment transport in the future will not be accounted for.
- **Aeolian sediment transport is not accounted for.** Most of the studied dunes were observed to be gaining sediment at some location (regardless of whether they were increasing or decreasing in overall volume), meaning that aeolian (wind-blown) sediment transport is contributing to their evolution. Accounting for regional variability in the supply and efficacy of wind-blown sand (a complex function of wind speed, wind direction, sediment moisture and beach width) requires applying or developing process-based aeolian sediment transport models which will help improve our ability to predict how dunes will evolve in the future.
- **Changes in wave climate are not accounted for.** Future changes in wave climate are poorly understood at present, but current Environment Agency guidance is to account for a 10% increase in wave heights by the year 2100. The Bruun rule doesn't account for such changes in wave conditions, but other more recent modelling approaches do and will be applied during the MS4S project to test the sensitivity of future dune predictions to a range of wave climate scenarios.

While the observed behaviour of the dune systems in this report is likely to be indicative of future dune behaviour, the predicted magnitudes of dune change should be considered as preliminary estimates only. A number of the above limitations will be addressed during the MS4S project through the use of more complex numerical models that have become available in recent years. These will provide improvements to the 'traditional' Bruun rule approach applied in this report and are expected to yield more reliable and site-specific forecast of future dune dynamics.

4. Conclusion

Over the survey period (2007/09 to 2019/20) about half of the forty sites included in the MS4S project have lost volume and half have gained volume, while the majority of sites (58%) have retreated. Most sites, however, do not have a statistically significant trend in both dune toe position change (δX) and dune sediment volume change (δQ) over time, with only eight dune sites having a significant trend in both. For these eight sites, correlation is seen between the rate at which the dune is advancing/retreating ($\delta X/\delta T$) and the rate at which the dune is gaining/losing sediment ($\delta Q/\delta T$) suggesting that, in general, dunes that retreat quickly, lose volume quickly, and vice versa. However, at one location (Summerleaze) the dune is gaining volume, while also retreating. Therefore, three distinct responses are observed:

1) Dunes that are gaining sediment and advancing, which are likely dominated by aeolian (wind-driven) sediment transport from the beach into the dunes (n = 3)
2) Dunes that are losing sediment and retreating, which are likely dominated by storm erosion (n = 4)
3) Dunes that are gaining sediment and retreating, referred to as roll-over, which are likely dominated by storm erosion of the frontal dune and aeolian sediment transported from the beach and the front of the dune to the top and back of the dune (n =1)

In fact, more than half the dunes show signs of rollover through sediment gains on top of the dune, but in many cases this is outpaced by erosion of the dune front, placing them into the second mode of response listed above. At other sites, the dune is losing sediment at one end of the frontage but gaining sediment at the other end.

Future projections of dune evolution have been made by extrapolating contemporary dune toe changes and by making Bruun rule projections. At several sites with a statistically significant trend in δX, extrapolation of current trends leads to estimates of dune toe retreat/advance by 2100 in excess of 100 m. While the observed behaviour of the dune systems over the past 12 years reflects real, contemporary dune dynamics, this behaviour is not necessarily a reliable indicator of future dune dynamics, as the trends may not be sustained indefinitely. Application of the Bruun rule predicts a retreat of the dune systems by 2100 ranging from 13 m to 61 m. There are many assumptions associated with the Bruun rule and its applicability for predicting shoreline retreat due to sea-level rise is widely debated in the international coastal literature. Some of the general criticism has been addressed in this report through using site-specific factors, including dune height and local wave conditions, as well as considering the uncertainties associated with the forecasts through application of a probabilistic approach. Therefore, we consider the Bruun rule forecasts of dune retreat, with the associated uncertainties, as a useful first approximation of the effect of sea-level rise on the different dune sites on the Cornish coast shoreline. However, during the remainder of the MS4S project we also recognise the

need to improve these projections by developing models that explicitly account for (a) sediment availability (sources and sinks, and depth to bedrock), (b) aeolian sediment transport, and (c) storm wave erosion.

References

Battjes, J. A. (1974). Surf similarity. In *Coastal Engineering 1974* (pp. 466-480).

Birkemeier, W.A., (1985). Field data on seaward limit of profile change. *Journal of Waterway, Port, Coastal and Ocean Engineering*, 111 (3), 598-602.

Brooke, B. P., Huang, Z., Nicholas, W. A., Oliver, T. S., Tamura, T., Woodroffe, C. D., & Nichol, S. L. (2019). Relative sea-level records preserved in Holocene beach-ridge strandplains–An example from tropical northeastern Australia. *Marine Geology*, *411*, 107-118.

Bruun, P. (1954). *Coast erosion and the development of beach profiles* (Vol. 44). US Beach Erosion Board.

Burvingt, O., & Castelle, B. (2023). Storm response and multi-annual recovery of eight coastal dunes spread along the Atlantic coast of Europe. *Geomorphology*, *435*, 108735.

Capobianco, M., Larson, M., Nicholls, R. J., & Kraus, N. C. (1997, June). Depth of closure: A contribution to the reconciliation of theory, practice, and evidence. In *Coastal Dynamics' 97* (pp. 506-515). ASCE

Cooper, J. A. G., Masselink, G., Coco, G., Short, A. D., Castelle, B., Rogers, K., ... & Jackson, D. W. T. (2020). Sandy beaches can survive sea-level rise. *Nature Climate Change*, *10*(11), 993-995.

Cooper, J. A. G., & Pilkey, O. H. (2004). Sea-level rise and shoreline retreat: time to abandon the Bruun Rule. *Global and planetary change*, 43(3-4), 157-171.

Davidson-Arnott, R. G., & Bauer, B. O. (2021). Controls on the geomorphic response of beach-dune systems to water level rise. Journal of Great Lakes Research, 47(6), 1594-1612.

Hallermeier, R. J. (1980). A profile zonation for seasonal sand beaches from wave climate. *Coastal Engineering*, *4*, 253-277.

Hird, S., Stokes, C., & Masselink, G. (2021). Emergent coastal behaviour results in extreme dune erosion decoupled from hydrodynamic forcing. *Marine Geology*, *442*, 106667.

Karunarathna, H., Brown, J., Chatzirodou, A., Dissanayake, P., & Wisse, P. (2018). Multi-timescale morphological modelling of a dune-fronted sandy beach. *Coastal Engineering*, *136*, 161-171.

Masselink, G., Brooks, S., Poate, T., Stokes, C., & Scott, T. (2022). Coastal dune dynamics in embayed settings with sea-level rise–Examples from the exposed and macrotidal north coast of SW England. *Marine Geology*, 106853.

Masselink, G., Scott, T., Poate, T., Russell, P., Davidson, M., & Conley, D. (2016). The extreme 2013/2014 winter storms: hydrodynamic forcing and coastal response along the southwest coast of England. *Earth surface processes and landforms*, *41*(3), 378-391.

Nicholls, R. J., Birkemeier, W. A., & Hallermeier, R. J. (1996). Application of the depth of closure concept. In *Coastal Engineering 1996* (pp. 3874-3887).

Palmer, M., Howard, T., Tinker, J., Lowe, J., Bricheno, L., Calvert, D., Edwards, T., Gregory, J., Harris, G., & Krijnen, J. (2018). UKCP18 marine report.

Rosati, J. D., Dean, R. G., & Walton, T. L. (2013). The modified Bruun Rule extended for landward transport. *Marine Geology*, *340*, 71-81.

Radley, G. P. (1994). *Sand Dune Vegetation Survey of Great Britain: A national inventory* (Vol. Part 1 : England). Joint Natur Conservation Comittee.

Ruessink, B., & Jeuken, M. (2002). Dunetoe dynamics along the Dutch coast. *Earth Surface Processes and Landforms: The Journal of the British Geomorphological Research Group*, *27*(10), 1043-1056.

Stockdon, H. F., Holman, R. A., Howd, P. A., & Sallenger Jr, A. H. (2006). Empirical parameterization of setup, swash, and runup. *Coastal Engineering*, *53*(7), 573-588.

Thom, B. G. (1984). Transgressive and regressive stratigraphies of coastal sand barriers in southeast Australia. *Marine Geology*, *56*(1-4), 137-158.

van IJzendoorn, C. O., de Vries, S., Hallin, C., & Hesp, P. A. (2021). Sea level rise outpaced by vertical dune toe translation on prograding coasts. *Scientific Reports*, *11*(1), 1-8.

Wiggins, M., Scott, T., Masselink, G., Russell, P., & Mccarroll, R. J. (2019). Coastal embayment rotation: Response to extreme events and climate control, using full embayment surveys. *Geomorphology*, *327*, 385-403. https://doi.org/10.1016/j.geomorph.2018.11.014

Appendix A. LiDAR data collection years

Table A-1. First and last LiDAR survey dates.

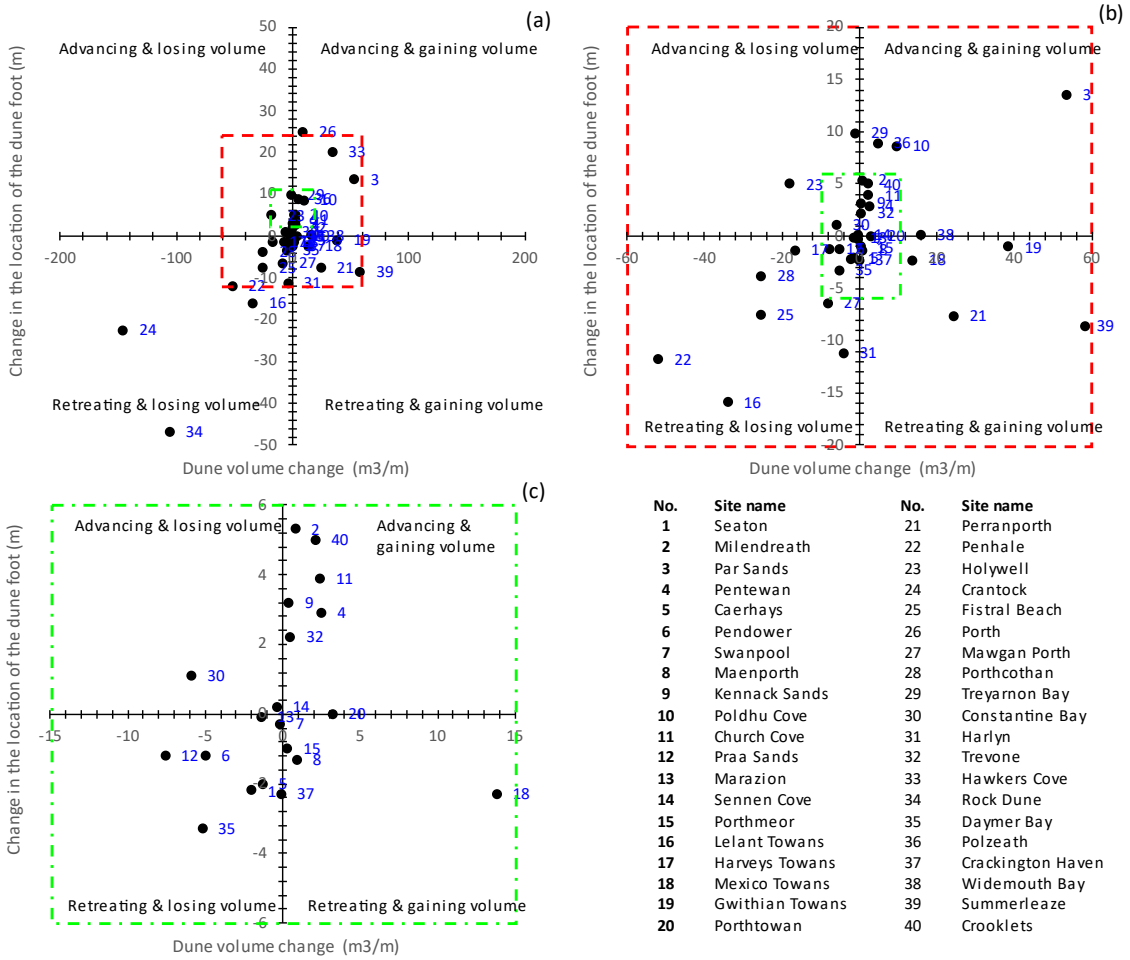
Site Name	LiDAR first year	LiDAR last year
Southern Coast		
Seaton	09/02/2008	17/09/2020
Milendreath	09/02/2008	17/09/2020
Par Sands	24/01/2008	17/09/2020
Pentewan	31/03/2007	17/09/2020
Caerhays	17/04/2007	19/04/2019
Pendower	17/04/2007	19/04/2019
Swanpool	17/04/2007	19/04/2019
Maenporth	17/04/2007	19/04/2019
Kennack Sands	27/09/2007	19/04/2019
Poldhu	27/09/2007	21/02/2019
Church Cove	27/09/2007	21/02/2019
Praa Sands	17/04/2007	21/02/2019
Marazion	17/04/2007	21/02/2019
Northern Coast		
Sennen	11/02/2008	17/09/2020
Porthmeor	09/03/2008	17/09/2020
Lelant Towans	09/03/2008	17/09/2020
Harveys Towans	09/03/2008	17/09/2020
Mexico Towans	09/03/2008	17/09/2020
Gwithian Towans	09/03/2008	17/09/2020
Porthtowan	09/03/2008	18/04/2019
Perranporth	10/02/2008	26/11/2020
Penhale	10/02/2008	26/11/2020
Holywell	10/02/2008	26/11/2020
Crantock	10/03/2009	26/11/2020
Fistral Beach	09/03/2008	26/11/2020
Porth	09/03/2008	26/11/2020
Mawgan Porth	09/03/2008	18/04/2019
Porthcothan	09/03/2008	18/04/2019
Treyarnon Bay	09/03/2008	18/04/2019
Constantine Bay	09/03/2008	18/04/2019
Harlyn	10/02/2008	18/04/2019
Trevone	10/02/2008	18/04/2019
Hawkers Cove	10/02/2008	26/11/2020
Rock Dune	10/02/2008	26/11/2020
Daymer Bay	10/02/2008	26/11/2020
Polzeath	10/02/2008	18/04/2019
Crackington Haven	24/04/2007	18/04/2019
Widemouth	30/03/2007	18/04/2019
Summerleaze	30/09/2007	18/04/2019
Crooklets	30/09/2007	18/04/2019

Appendix B. 2100 Projected Retreat using Contemporary Rates and the Bruun Rule

Table B-1. Values of the estimated 2100 retreat using the two contemporary rate estimates ($\delta X/\delta T$ and $\delta X_{last-first}/\delta T$) and using the Bruun rule. Sites with statistically significant advancing trends are highlighted in blue and those with statistically significant retreating trends in red.

Site Name	Estimated 2100 retreat by extrapolating δX/ δT (m)	Estimated 2100 retreat by extrapolating $\delta X_{last-first}/ \delta T$ (m)	Estimated Bruun retreat in 2100 (m)
Southern Coast			
Seaton	-10	-14	-26
Milendreath	42	34	-23
Par Sands	100	86	-61
Pentewan	3	17	-19
Caerhays	-7	-14	-31
Pendower	-18	-8	-21
Swanpool	-2	-2	-19
Maenporth	2	-9	-35
Kennack Sands	-19	23	-15
Poldhu	58	61	-25
Church Cove	25	27	-23
Praa Sands	-6	-8	-13
Marazion	1	-1	-33
Northern Coast			
Sennen	-1	1	-18
Porthmeor	-12	-6	-23
Lelant Towans	-73	-101	-33
Harveys Towans	-26	-8	-33
Mexico Towans	-15	-15	-13
Gwithian Towans	-12	-6	-24
Porthtowan	7	0	-24
Perranporth	-35	-48	-25
Penhale	-62	-74	-18
Holywell	24	31	-17
Crantock	-188	-153	-23
Fistral Beach	-41	-47	-22
Porth	150	157	-47
Mawgan Porth	-38	-47	-40
Porthcothan	-72	-27	-31
Treyarnon Bay	63	72	-35
Constantine Bay	-5	8	-25
Harlyn	-93	-81	-21
Trevone	-3	16	-27
Hawkers Cove	162	126	-57
Rock Dune	-67	-292	-15
Daymer Bay	-29	-21	-28
Polzeath	55	64	-47
Crackington Haven	-10	-15	-27
Widemouth	-6	2	-26
Summerleaze	-93	-60	-27
Crooklets	22	35	-31

Appendix C. Changes in dune volume and dune foot position observed over the survey period (2007/2009 to 2019/2020)



No.	Site name	No.	Site name
1	Seaton	21	Perranporth
2	Milendreath	22	Penhale
3	Par Sands	23	Holywell
4	Pentewan	24	Crantock
5	Caerhays	25	Fistral Beach
6	Pendower	26	Porth
7	Swanpool	27	Mawgan Porth
8	Maenporth	28	Porthcothan
9	Kennack Sands	29	Treyarnon Bay
10	Poldhu Cove	30	Constantine Bay
11	Church Cove	31	Harlyn
12	Praa Sands	32	Trevone
13	Marazion	33	Hawkers Cove
14	Sennen Cove	34	Rock Dune
15	Porthmeor	35	Daymer Bay
16	Lelant Towans	36	Polzeath
17	Harveys Towans	37	Crackington Haven
18	Mexico Towans	38	Widemouth Bay
19	Gwithian Towans	39	Summerleaze
20	Porthtowan	40	Crooklets

Figure C-1. Changes in dune volume (x-axis) and location of the dune foot (y-axis) extracted between the first available LiDAR survey (2007 to 2009 depending on the site) and last available LiDAR data (2019 to 2020 depending on the site). a). all sites; b). same plot zoomed in to the area highlighted by the red, dashed line rectangle in (a). c). same plot zoomed in to the area highlighted by the green, dash-dot line rectangle in (a) and (b). The dates of the first and last LiDAR data available are provided in Table A-1 and the corresponding dune foot change and volume change values are included in Table 3-1.